Geomorphology 466 (2024) 109446

Contents lists available at ScienceDirect

Geomorphology

journal homepage: www.journals.elsevier.com/geomorphology

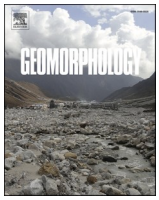

Geomorphic characteristics influencing post-fire river response in mountain streams

Shayla Triantafillou *, Ellen Wohl

Department of Geosciences, Colorado State University, Fort Collins, CO, United States

ARTICLE INFO

Keywords:
Wildfire
Resilience
Debris flow
Large wood
Logjams
Heterogeneity
Geomorphic hazards
Rocky Mountains
Disturbance

ABSTRACT

As wildfires increase in frequency and severity, there is a growing interest in understanding river response to the wildfire disturbance cascade. Numerous headwater mountain catchments within the Cache la Poudre (Poudre) River basin in the Colorado Front Range, USA burned severely and extensively during the 2020 Cameron Peak fire. Debris flows and flash floods occurred in many of these catchments triggered by convective storms after the fire. The downstream effects of the floods and sediment varied along a continuum from attenuated and largely contained within the catchment, to releasing substantial volumes of water and sediment to the Poudre River. We conceptualize these catchments as exhibiting decreasing absorbance of post-fire disturbance along the continuum described above based on the geomorphic evidence of relative sediment export. We conceptualize characteristics on different spatial scales as driving or resisting response to disturbance and therefore impacting the absorbing capacity (ability to attenuate post-fire fluxes) of the catchment. As the magnitude of resisting characteristics increases at the catchment, inter- and intra- reach scales, we hypothesize that a catchment will increasingly absorb the impacts of the wildfire disturbance cascade. We conducted longitudinally continuous surveys to measure reach-scale characteristics within each study catchment. We focus on the catchment- and reach-scale geomorphic, vegetation, and burn characteristics. The floods observed at the study catchments illustrate fire influencing the elevation above which rainfall-induced flooding occurs due to the efficient conveyance of water from hillslopes to channels after wildfire. Results suggest that inter- and intra-reach spatial heterogeneity are better aligned with absorbance capacity than catchment-scale characteristics: greater absorbing capacity is associated with greater longitudinal variations in floodplain/channel width and more reaches with wide floodplains, low channel gradients, beaver-modified topography, and multi-stem deciduous vegetation. We connect the capacity to absorb the impacts of disturbance as informing the catchment response to wildfire disturbance.

1. Introduction

As climate change is projected to increase wildfire frequency and severity across the western United States (Westerling et al., 2006; Dennison et al., 2014; Abatzoglou and Williams, 2016; Abatzoglou et al., 2017, 2018), understanding the characteristics that promote catchment resilience post-fire is critical to protect water resources that are impacted by fire (Murphy et al., 2018). This view is guided by principles of disturbance, thresholds, and recovery in terms of equilibrium (Thorn and Welford, 1994). Our concept of geomorphic resilience includes the capacity of a system to absorb disturbances, as is the emergent view recently (Thoms et al., 2018; Fuller et al., 2019). In these ways, the concept of resilience is inherent in the assumptions and theories upon which fluvial geomorphology is built (Fuller et al., 2019; Piégay et al., 2020). Walker et al. (2004) define resilience as the capability of a system to absorb disturbance while undergoing change so as to still retain essentially the same function, structure, identity, and feedbacks. Catchments likely exhibit differing resilience post-fire that varies within and between catchments in relation to biogeomorphic characteristics (Roth et al., 2022; Wohl et al., 2022; Corenblit et al., 2024; Wohl et al., 2024a, 2024b). Our primary objective is to describe a range of resilience and evaluate the relative influence of reach- and catchment-scale characteristics in forested montane rivers of the Colorado Front Range, USA on catchment response to wildfire disturbance. From this point forward, we refer to resilience as absorbing capacity to differentiate our focus on post-fire response from other definitions and measures

* Corresponding author.
E-mail address: shayla.triantafillou@colostate.edu (S. Triantafillou).

https://doi.org/10.1016/j.geomorph.2024.109446
Received 19 July 2024; Received in revised form 26 September 2024; Accepted 28 September 2024
Available online 3 October 2024

of resilience.

1.1. Wildfire disturbance cascade

Wildfires initiate a disturbance cascade. The impacts of fire on the hillslope are transferred to the river corridor because of the connection between valley floor and adjacent hillslopes (Davis, 1898; Hynes, 1975), so that wildfires affect hydrology, water quality, and geomorphology in river corridors (Tiedemann et al., 1979; Minshall et al., 1989; Mast and Clow, 2008; McGuire and Youberg, 2019). High severity fires combust organic matter, reducing ground cover and changing hillslope roughness, evapotranspiration, and runoff generation (Blount et al., 2020). High temperatures also alter soil structures, increasing water repellency and decreasing infiltration rates (DeBano, 2000; Martin and Moody, 2001; Wieting et al., 2017). Across the landscape, burned hillslopes have lower erosion thresholds and therefore increased erosion depending on precipitation characteristics (Moody and Martin, 2001; Wu et al., 2021; Noske et al., 2024). Moderate to high severity fire results in heightened sediment and water fluxes throughout burned catchments (Benavides-Solorio and MacDonald, 2001; Alessio et al., 2021), driving changes in river corridor characteristics on multiple spatial and temporal scales. Enhanced erosion response typically persists for up to five years in the Colorado Front Range (Martin and Moody, 2001; Moody, 2001; Ryan et al., 2024).

Debris flows are more likely to occur in catchments that have burned in the Intermountain West (e.g. Parrett, 1987; Meyer and Wells, 1997; Cannon, 2001; Parrett et al., 2004; Cannon and Gartner, 2005; Riley et al., 2013; McGuire et al., 2021) because wildfire increases flow and sediment transport relative to precipitation intensity. Unlike debris flows started by landslides, post-fire debris flows are triggered by exceedance of a rainfall intensity-duration threshold. Studies from diverse areas indicate that these events derive sediment from within the channel via lateral and vertical erosion (Santi et al., 2008) and from the hillslopes (DiBiase and Lamb, 2020; Rengers et al., 2021). There is commonly no initiation point and these debris flows can occur with little antecedent moisture (Cannon et al., 2008). The storms that trigger these debris flows in Colorado are typically short in duration, triggering debris flows within minutes to hours of rainfall, and high in intensity (Cannon et al., 2008).

1.2. Resilience

The characteristics affecting the magnitude of response to post-fire disturbance span multiple spatial scales from catchment to reach (Fig. 1). We define a reach as a continuous length of river corridor with consistent valley and channel geometry and land cover. Reaches are typically tens to hundreds of meters in length in the 3rd-order catchments examined here.

We conceptualize biogeomorphic characteristics as driving or resisting response to disturbance. Driving characteristics that influence erosional force, such as higher channel gradient, magnify the response to disturbance by facilitating more efficient conveyance of fluxes. Resisting characteristics promote attenuation of fluxes, resulting in greater absorbing capacity after disturbance. This conceptualization provides a framework for comparing characteristics among burned catchments. When the influence of the driving characteristics exceeds that of the resisting, a system is more likely to shift states into an alternative stable state or an unstable transient state more prone to response to

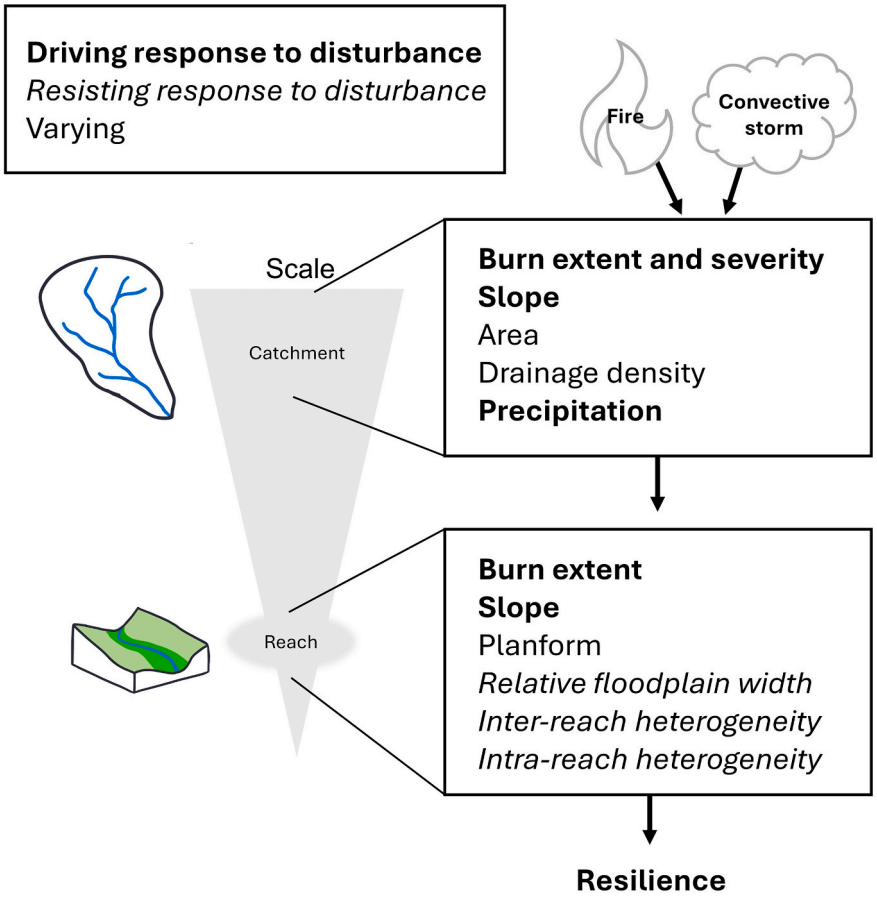

Fig. 1. Multi-scale characteristics influencing river corridor response to disturbance. Assuming an increase in the relative magnitude of the specified characteristic, each characteristic is categorized as either **driving** (bold) or *resisting* (italic) response to disturbance. The inverse is also implied to be true. Where characteristics could be driving or resisting response to disturbance depending on context, they are described as varying.

disturbance.

Wohl et al. (2022) conceptualize reach-scale flux attenuation as increasing absorbing capacity, or the capability to undergo change while retaining the same function, structure, and feedbacks on the catchment scale. Because total channel length of first- to third-order streams is cumulatively dominant (Downing, 2012), reach-scale attenuation in small streams must greatly influence the magnitude of the catchment-scale disturbance cascade initiated by wildfire. This suggests that catchment-scale absorbing capacity is greatly influenced by features that attenuate fluxes at the reach scale.

Reach-scale water and sediment flux attenuations are primarily driven by valley geometry, spatial heterogeneity of the river corridor, vegetation, and 3D connectivity within the river corridor (Wohl, 2016; Wohl et al., 2017, 2018). Reaches with less lateral confinement allow for more overbank flow, greater channel sinuosity, diverse floodplain topography, and formation of multithread channel planform, facilitating energy dissipation and associated sediment deposition (e.g. Pang, 1998; Naiman et al., 2005; Entwistle et al., 2018).

Spatial heterogeneity in river corridors contributes to absorbing capacity by attenuating downstream fluxes of water and sediment (Wohl, 2016), commonly by increasing hydraulic roughness of the channel and floodplain, obstructing flow, decreasing longitudinal connectivity, and increasing lateral connectivity. Spatial heterogeneity can occur longitudinally (between reaches) and within a reach. Inter-reach heterogeneity increases as reaches alternate between wide, low gradient geometry and confined, high gradient geometry, called beads and strings, respectively (Stanford et al., 1996). Alternating reaches commonly differ in substrate, bedforms, planform, channel-floodplain connectivity, beaver-modified topography, and abundance of large wood and logjams. Beads contain greater amounts of heterogeneity elements on a local scale and therefore elements that promote absorbing capacity (Wohl et al., 2018, 2024b; Dunn et al., 2024). For example, beads contain disproportionately high volumes of large wood (Wohl, 2011), beaver-modified topography (Westbrook et al., 2006), and channel-hyporheic connectivity (Ader et al., 2021). Structural and functional heterogeneity created by beavers and in-channel wood is associated with more overbank flow, secondary channels, and lateral connectivity, all of which promote attenuation and contribute to absorbing capacity (Jones and Smock, 1991; Burchsted et al., 2010; Sear et al., 2010; Wohl, 2011; Collins et al., 2012; Polvi and Wohl, 2013; Livers and Wohl, 2016; Fairfax and Whittle, 2020; Marshall et al., 2021; Dunn, 2023). Spatial heterogeneity and flux attenuation can create a positive feedback, holding a system in a single, dynamic state rather than shifting to an alternative state when disturbed (Wohl et al., 2024b).

As landcover and climate change, wildfires continue to increase in frequency and severity (Bowman et al., 2009; Westerling et al., 2006; Dennison et al., 2014). Consequently, understanding and fostering the characteristics that promote catchment- and reach-scale absorbing capacity post-fire is critical for water resources and hazard mitigation in Colorado and other fire-prone regions. Although we understand the general interactions described above, there has been little work to quantitatively compare catchments that represent a range of responses to wildfire disturbance, or to quantify the spatial distribution, types, and levels of heterogeneity that create absorbing capacity. These issues are of critical importance as communities in fire-prone regions strive to implement pre- and post-fire landscape management designed to enhance resilience to wildfire disturbances. Post-fire management in the study region ranges from catchment-scale efforts including applying mulch, seeding hillslopes, and replanting trees to the reach-scale installation of in-channel structures. In-channel structures include replanted riparian vegetation, especially willow (*Salix* spp.), check dams, log jams, and beaver mimicry structures to retain sediment after wildfire (Graham, 2003; Pollock et al., 2007).

Our primary objective is to evaluate the relative influence of reach- and catchment-scale characteristics on response to disturbance. We assess the following hypotheses that catchments with lesser response to disturbance will have:

i. more resisting characteristics and fewer driving characteristics at the catchment scale
ii. greater inter-reach heterogeneity
iii. more resisting characteristics and fewer driving characteristics at the reach scale

This analysis is based on region-specific data, but the concepts and approach are applicable to other high-relief and fire-prone catchments.

2. Study area

The study area is in the Southern Rocky Mountains in the northern Front Range of Colorado, USA. The seven catchments within the study area are headwater tributaries to the Poudre River (Fig. 2). These catchments burned in the Cameron Peak fire in 2020, which burned 845 km^2 (208,913 acres). Over 40 % of the burned area was classified as being burned at moderate to high severity (USDA Forest Service, 2020). Prior to this fire, these sites had not burned for more than a century (National Interagency Fire Center, 2022).

The region is underlain primarily by Precambrian- and Proterozoic-aged granitoids and gneisses (Green, 1992; Horton, 2017). The study sites were not glacially modified during the Pleistocene (Madole et al., 1998). Most of the study catchments by area are between 2300 and 3250 m elevation. In the summer, mountainous parts of Colorado have frequent thunderstorms (Jarrett, 1993) that cause flash flooding in unburned catchments below 2300 m (Hansen et al., 1978; Jarrett, 1990).

The study sites are ungauged tributaries, but the U.S. Geological Survey maintains a stream gauge at Rustic, CO in the Poudre River catchment that indicates that annual peak runoff occurs during late spring snowmelt. Gauge data from the first year after the fire at Little Beaver Creek show peak runoff occurring during spring snowmelt, but indicate that convective summer storms also caused high, peaked flows (White et al., 2022; Wohl et al., 2022). The floods initiated by convective storms do not comprise a seasonally recurrent part of the hydrograph, but they cause flashy and spatially discontinuous flooding, erode sediment, and initiate mass movements. Convective storms have the capacity to initiate substantial geomorphic change within burned tributary catchments, and the impacts of these local events have been observed outside of these catchments in downstream river corridors (Grimm et al., 1995).

Landcover consists of coniferous, montane forests between 2100 and 2750 m elevation and subalpine forests between 2600 and 3650 m (Chapman et al., 2006). Montane forest has an overstory dominated by ponderosa pine (*Pinus ponderosa*) and Douglas-fir (*Pseudotsuga menziesii*) with pockets of aspen (*Populus tremuloides*). Subalpine forests are dominated by lodgepole pine (*Pinus contorta*), Engelmann spruce (*Picea engelmannii*), and subalpine fir (*Abies lasiocarpa*). Riparian areas include a variety of willow species (*Salix* spp.), thinleaf alder (*Alnus incana*), and river birch (*Betula occidentalis*) (Malone et al., 2019). Although fire is a natural disturbance over millennia (Minckley et al., 2012), decades of fire suppression in the western US have resulted in more vegetation in the understory and denser, evenly aged forests (Veblen and Donnegan, 2005; Veblen and Lorenz, 1986). Today, the single largest driver of forest loss in the northern Front Range is wildfire (Rodman et al., 2019).

2.1. Storm and flood events

Following the Cameron Peak fire in 2020, a series of convective storms over the summers of 2021 and 2022 triggered floods and debris flows across the burn scar. On 20 July 2021, a convective storm caused flooding and multiple debris flows at Black Hollow (BH), Sheep Creek (SC), and Sheep Gulch (SG). Rain gauges located near the center of intense precipitation recorded peak 15-min rainfall intensities of 36.6 and 51.8 mm/h, respectively, exceeding the threshold to trigger debris

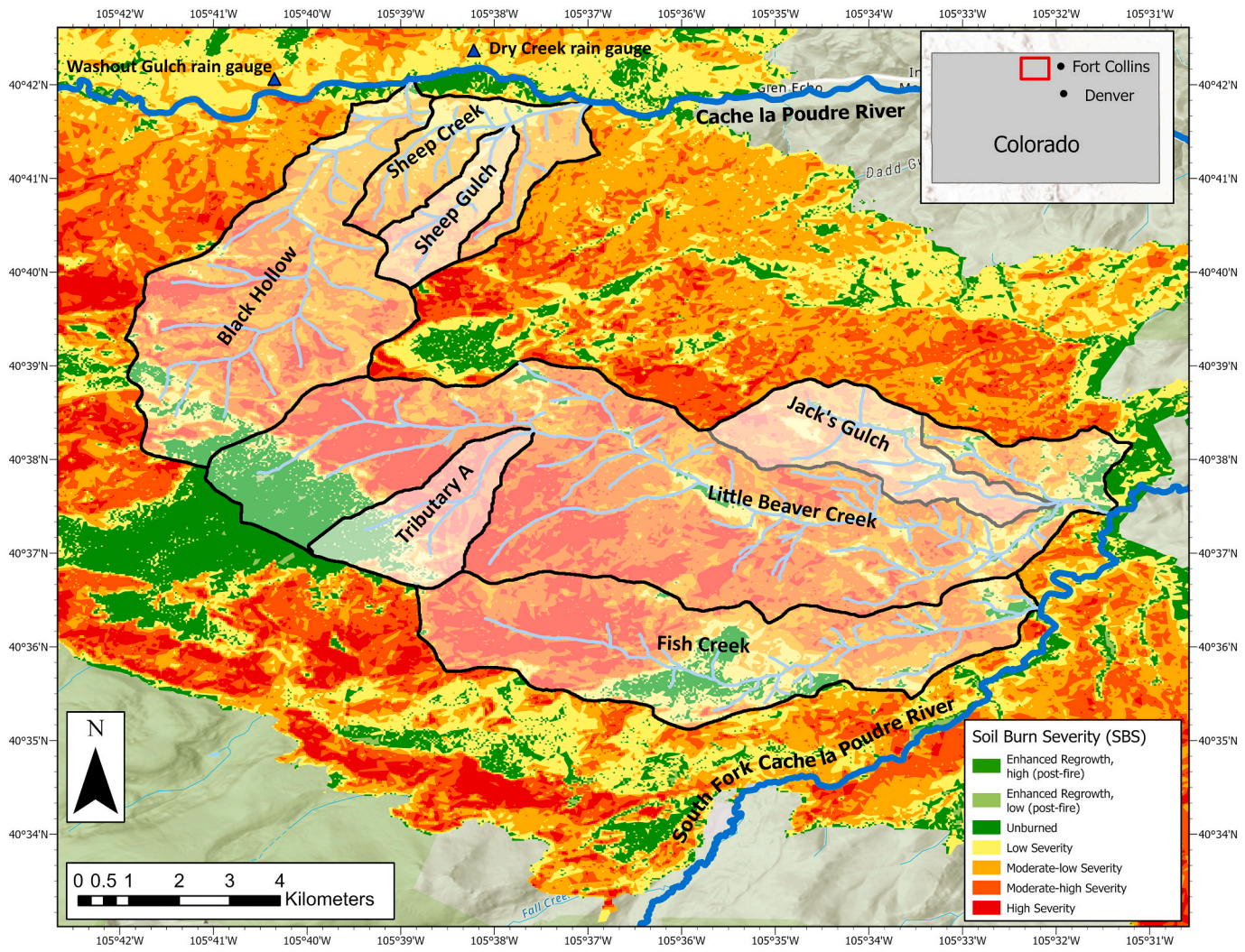

Fig. 2. Map of seven study catchments and their location within Colorado. All study catchments were within the burn scar of the 2020 Cameron Peak fire. The soil burn severity of the study catchments is also depicted (Woodward and Vorster, 2022). Little Beaver Creek Tributary A and Jack's Gulch are within the Little Beaver Creek catchment. Sheep Gulch is within the Sheep Creek catchment. Blue triangles represent publicly available rain gauges.

flows of 33.2 mm/h modeled for the entire burn scar (Kostelnik et al., 2022). The 20 July 2021 event resulted in the destruction of property, damage to the roadway and bridge, fish kill, deteriorated water quality, extensive sedimentation on a fan, and four fatalities (Kostelnik et al., 2022). A convective storm the following year on 15 July, 2022 resulted in flooding across Fish Creek (FC), Jack's Gulch (JG), Little Beaver Creek (LBC), and Tributary A (LBCA) (Wohl et al., 2024a). We observed in the field that debris flows triggered by these events appear to have been generated by sediment entrainment through surface runoff rather than shallow landslides, a scenario that is common in unburned settings (Cannon and Gartner, 2005).

3. Methods

The catchments selected for this study are all headwaters in the Poudre River drainage basin that burned during the 2020 Cameron Peak fire. We selected sites to have comparable burn characteristics, elevations, bedrock geology, glacial history, and known convective storms following the Cameron Peak fire. We assigned each catchment to a category representing the relative response to disturbance a priori using a field-based qualitative assessment of geomorphic indicators relating to sediment export during summer convective storms. A catchment with a large debris or alluvial fan at the channel outlet was ranked as having the greatest sediment export and therefore absorbed the impacts of disturbance the least. A catchment that had no evidence of scour and deposition resulting from a large flood was ranked as the least impacted by the wildfire disturbance cascade and therefore had the greatest absorbing capacity. Where data availability allowed, we quantitatively constrained the amount of sediment export from the catchment using repeat digital elevation models. See Table 1 for a summary of methods.

3.1. Field methods

We conducted longitudinal reach surveys within each study catchment. We followed the river downstream from the channel head, defining the boundaries between reaches by field-observed relative valley and channel geometry using a Garmin GPSMAP 66st and a Garmin eTrex10 with 3-m horizontal accuracy. Within each reach we documented burn status, vegetation type, basal area of floodplain or adjacent forest, channel planform (maximum number of channels, or channel count), channel bedform, bankfull width, floodplain width, number of channel and floodplain jams, and number of beaver berms.

Burn status was documented categorically in the field as burned, unburned, or mixed. Vegetation type was noted categorically as conifer, willow, aspen, or herbaceous based on the species present, where herbaceous denoted a lack of trees rather than implying that there was no

Table 1
Summary of methods and data products.

Methods	Data Product(s)
Field survey	• Absorbing capacity ranking of each catchment • Reach boundaries • Geomorphic characteristics o Channel width o Floodplain width o Planform o Presence of beaver modified topography • Vegetation o Categorical floodplain vegetation type o Basal area o Channel jam density o Floodplain jam density • Burn characteristics o Burn status
Geospatial analyses	• Geomorphic catchment characteristics o Area o Mean catchment slope o Elongation ratio o Relief ratio o Drainage density o Concavity index • Vegetation catchment characteristics o Normalized Difference Vegetation Index (NDVI) • Burn characteristics o Burn extent o Burn severity • Precipitation o 15-min precipitation intensity
Statistical analyses	• Hypothesis testing • Descriptive regression models
Sensitivity analyses	• Geomorphic change during events

herbaceous vegetation where other species were present. Basal area of the river corridor forest was measured with a Panama Angle Gauge at approximately one channel width away from bankfull. All standing trees (living and dead) were included. Channel planform and channel bedform were determined categorically. Bankfull channel, floodplain widths, and high-water marks indicative of the most recent spring snowmelt flows were measured using a Laser Technology TruPulse 360B laser range finder with ±0.1 m accuracy. Logjams were designated as at least three pieces of wood in contact, with each piece of wood at least 1 m in length and 10 cm in diameter. Jams within the bankfull channel were tallied as channel jams. Jams outside of the bankfull channel but within the bounds of high-water marks were tallied as floodplain jams. The presence of beaver berms was tallied within each reach where clearly defined individual berms existed. Where there were complex beaver meadows, beaver-modified terrain was noted as "beaver meadow," indicating numerous, closely spaced berms throughout the length of the reach.

3.2. Remote methods

Catchment-scale and reach-scale characteristics that utilized geospatial data to quantify elevation, burn characteristics, and vegetation characteristics were evaluated using remote data and methods. These metrics were categorized as geomorphic, burn, vegetation, and precipitation characteristics. We used repeat lidar to calculate a DEM of difference within the river corridor to quantify minimum sediment export from Black Hollow. DEMs were available and adequately spatially aligned from 2020 and 2021 with 1/3 arc-second spatial resolution (Supplemental Information).

To consider catchment shape, elongation ratio was calculated as the ratio between the diameter of a circle encompassing the area of each catchment and the maximum catchment length (Schumm, 1956). To account for the shear stress exerted by runoff, we calculated relief ratio as the difference between the highest and lowest points of each catchment divided by the length of the longest National Hydrography Dataset (NHD) flowpath (Hydrologic Engineering Center, 2023). To quantify the network configuration, we calculated drainage density as the total NHD flowpath length in each catchment divided by the catchment area (Horton, 1932). We calculated the elevation of each reach boundary using the field-determined reach boundaries and the USGS 3DEP 1/3 arc second DEM. The channel gradient of each reach was calculated using the elevation and the NHD stream distance between each reach boundary. We calculated the concavity index as the ratio between the area under the longitudinal profile to the area under the normalized straight-line distance.

Burn characteristics of each catchment were calculated using a Soil Burn Severity dataset (Woodward and Vorster, 2022). To capture burn characteristics of each catchment and reach, we calculated the total proportion burned at any severity (burn extent) and the percentage of each area burned at moderate-high and high severities (burn severity). We calculated these metrics for each catchment's total area and for each reach using a 50-m lateral buffer from each stream segment. We quantified the precipitation over the study catchments during discrete storm events using Multiple Radar/Multiple Sensor (MRMS) data with 1-km spatial and 2-min temporal resolution from the National Oceanic and Atmospheric Administration (NOAA). We applied the MRMS correction to precipitation rate data using the radar-based QPE and the gauge-and-precipitation-and climatology-merged QPE products. Because the MRMS QPEs are known to have higher errors in remote, mountainous areas, we elected to present pixel distributions over the storm durations and catchment areas (White et al., 2023). We summarized the precipitation characteristics with median and 95th percentiles of 15-min precipitation intensity to be robust to skew and overestimates of single pixel maximums.

3.3. Analytical methods

Statistical analyses were performed using R version 4.2.1. When testing reach-scale characteristic data for equality of variance, we used Levene's test in the car package in R (Fox and Weisberg, 2019). Where assumptions of normality and variance were met, we used an analysis of variance (ANOVA) to test the differences in reach-scale characteristics between catchments. When the assumption of normality was not met, we performed analyses on logarithmically transformed data. We tested the difference between catchments with an ANOVA and a Tukey Honest Significant Difference using the emmeans package (Searle et al., 1980; Lenth, 2023). Where the assumptions of normality and variance were not met, we used a non-parametric Kruskal-Wallis Rank Sum test to test the differences in reach characteristics between catchments and Dunn's test (Dunn, 1964) to perform pairwise comparisons between sites. All hypotheses were tested at the $\alpha = 0.05$ level.

We created two sets of Poisson regression models to understand the influences on channel and floodplain jam distribution density surveyed in the field. We fit six Poisson regression models with the number of jams in each reach as the outcome and site as the predictor variable with an offset of the bankfull channel area, and different combinations of additional predictor variables that describe the geomorphic, vegetation, and fire characteristics. We calculated the Akaike information criterion (AIC) to assess the model for each of the six models and select the best model for interpretation. The statistical significance of Poisson regression models was assessed at the $\alpha = 0.05$ level using a likelihood ratio test.

Where data were available reflecting the state of the river corridor prior to the fire, we use comparisons between pre- and post-event data to assess the feasibility of using post-flood data to make inferences about the identity of the study sites (Triantafillou, 2024).

4. Results

We ranked seven study catchments into four categories reflecting their response to disturbance and surveyed 150 reaches within those

catchments. Based on geomorphic indicators of relative sediment export, Black Hollow absorbed disturbance the least and Jack's Gulch absorbed disturbance the most (Fig. 3, Fig. SI-1). A debris-fan 100-m wide formed at the junction of Black Hollow and the Poudre River. Boulders and large wood were transported and deposited at the outlet of the catchment, destroying property, and causing channel avulsion. Sediment from the event caused fish kill from the upper Poudre Canyon for almost 100 stream kilometers downstream (Battige, 2022). At the time of these analyses, repeat lidar-derived DEM data available at Black Hollow show 100,000 m^3 of sediment eroded, or 5780 m^3km^{-2} catchment area. This large amount of sediment export supports the classification of Black Hollow as having the largest magnitude of response to disturbance.

Sheep Creek and Tributary A within Little Beaver Creek had moderate debris fans at their outlets. The debris fans changed the form of these river corridors but did not significantly or persistently alter the form of the mainstem channels into which they drained. There was erosion and incision throughout the river corridors at these sites, indicating that the material deposited at the outlet was derived from the channel and floodplain. Fish Creek, Little Beaver Creek and Sheep Gulch had large floods with no fan at their outlets. There was flooding within these catchments as evidenced by erosion, but the absence of a depositional fan at the outlet indicated that the impacts of the flood were absorbed within each catchment. Jack's Gulch had no geomorphic evidence of sediment export and there was no evidence of major sediment redistribution throughout the catchment, supporting the classification of Jack's Gulch as having no large flood. In reporting results related to these relative rankings, we will refer to Black Hollow, Sheep Creek, and Little Beaver Creek Tributary A as sites with less capacity to absorb disturbance and Fish Creek, Little Beaver Creek, Sheep Gulch, and Jack's Gulch as having greater capacity to absorb disturbance.

4.1. Catchment characteristics

There are no apparent trends in any individual geomorphic, vegetation, or burn characteristics among the catchments (Table 2, Supplementary Information Table SI-1, Fig. SI-2, Fig. SI-3). This likely reflects the spatial heterogeneity associated with the wildfire, which covered an extensive area that included large portions of each of the study catchments.

Geomorphically significant precipitation events over the study catchments were identified as beginning on 20 July 2021 at 1200 UTC at Black Hollow, Sheep Creek, and Sheep Gulch, or 15 July 2022 at 1700 UTC at Little Beaver Creek Tributary A, Fish Creek, Little Beaver Creek, and Jack's Gulch. Across each of the seven catchments, maximum 15-min precipitation rates over the storm duration ranged from 45.9 mm/h at Sheep Gulch to 148.9 mm/h Tributary A within Little Beaver Creek. There is a negative relationship between the median and 95th percentile of the 15-min precipitation intensity over storm duration and the catchment response (Fig. 4). Sheep Gulch, ranked as having "Large Flood," had the highest median and the second highest 95th percentile of 15-min precipitation intensity, 2.9 and 33.0 mm/h, respectively, and thus did not align with this trend (Supplementary Information Table SI-2).

4.2. Inter-reach characteristics

The variance of floodplain to channel width ratio differed between sites ($p = 0.03$). Little Beaver Creek had greater floodplain to channel width ratio variance than Black Hollow ($p < 0.001$), and lower variance than Sheep Gulch ($p = 0.04$) (Fig. 5). Black Hollow had lower variance than Sheep Gulch, Little Beaver Creek Tributary A, Fish Creek, and Jack's Gulch ($p < 0.001$ for all). Sheep Gulch had greater variance than Fish Creek ($p = 0.01$). Sheep Creek and Fish Creek had lower variance than Jack's Gulch ($p = 0.02$, $p = 0.01$).

4.3. Reach characteristics

Reach maximum channel count did not vary significantly between catchments. Reach slope varied between catchments ($p < 0.001$) (Fig. 6). The mean of reach slopes at Black Hollow is significantly greater than the means of Fish Creek, Jack's Gulch, and Little Beaver Creek ($p = 0.06$, 0.006). The mean of reach slopes at Fish Creek is greater than at Little Beaver Creek ($p = 0.001$) and smaller than at Little Beaver Creek

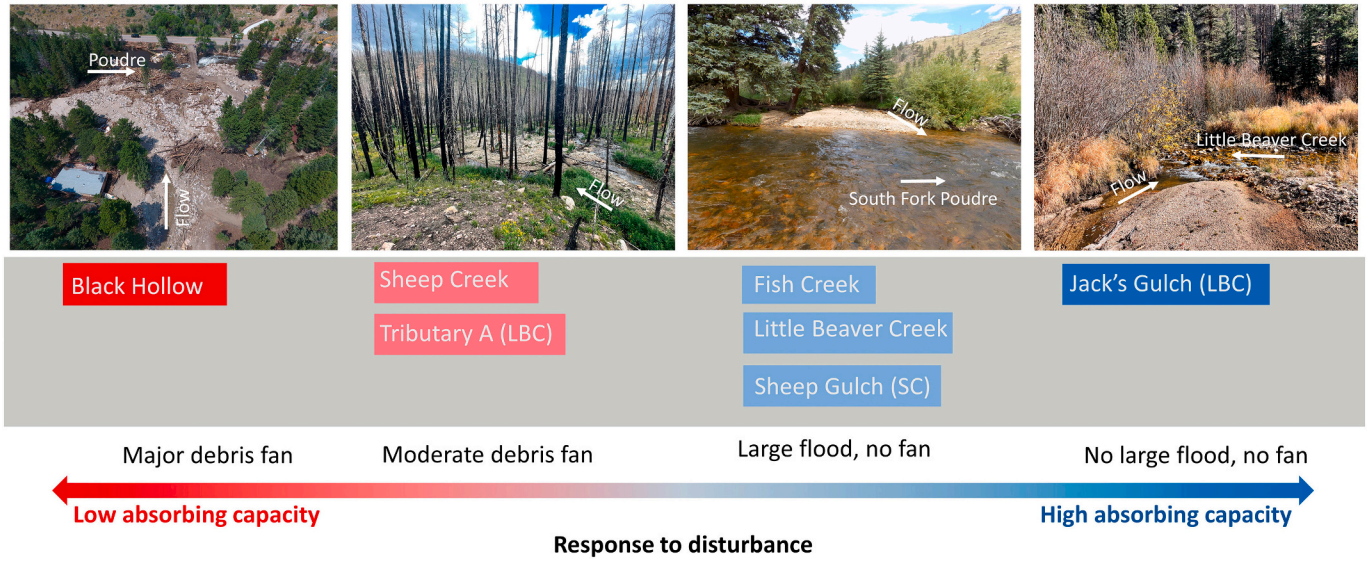

Fig. 3. Results of a priori ranking of seven study catchments on a scale of least to most disturbance absorption. Sites were ranked on a scale of absorbing capacity using post-event indicators of relative sediment export during storms and associated floods. The site with the lowest absorbing capacity, Black Hollow, had a large fan at the outlet, representing a large amount of sediment export, and was categorized as a "Major debris fan". The sites with the highest absorbing capacity with the least geomorphic impacts at the catchment outlet were Jack's Gulch within the Little Beaver Creek catchment. There was no evidence of sediment scour or deposition at the outlet, so Jack's Gulch was categorized as having "No large flood". The images taken in the field illustrate the impacts visible at the catchment outlets that were the basis for ranking. From left to right, the images are from Black Hollow, Tributary A (LBC), Little Beaver Creek, and Jack's Gulch. Additional photos of catchment outlets at Little Beaver Creek, Sheep Gulch, and Fish Creek are in Fig. SI-1. Far left image credit: U.S. Geological Survey.

Table 2
Catchment-scale geomorphic and burn characteristics across study sites.

Site	Area (km^2)	Elongation ratio	Mean basin slope (%)	Total stream length (km)	Drainage density	Relief ratio	Concavity index	Burn extent (%)	Burn severity (%)
Jack's Gulch	6.0	0.50	21.0	4.6	0.77	116	1.11	96	48.3
Fish Creek	17.1	0.50	10.3	9.2	0.54	105	0.72	90	52.7
Little Beaver Creek	37.6	0.55	9.7	27.2	0.72	76	0.74	90	59.8
Sheep Gulch	2.8	0.52	40.0	3.3	1.18	209	0.78	99	39.0
Sheep Creek	7.6	0.68	17.1	7.8	1.02	173	0.13	99	27.6
Tributary A	4.6	0.59	25.0	3.5	0.75	401	0.87	77	57.9
Black Hollow	17.3	0.56	14.5	9.7	0.56	159	0.91	99	49.5

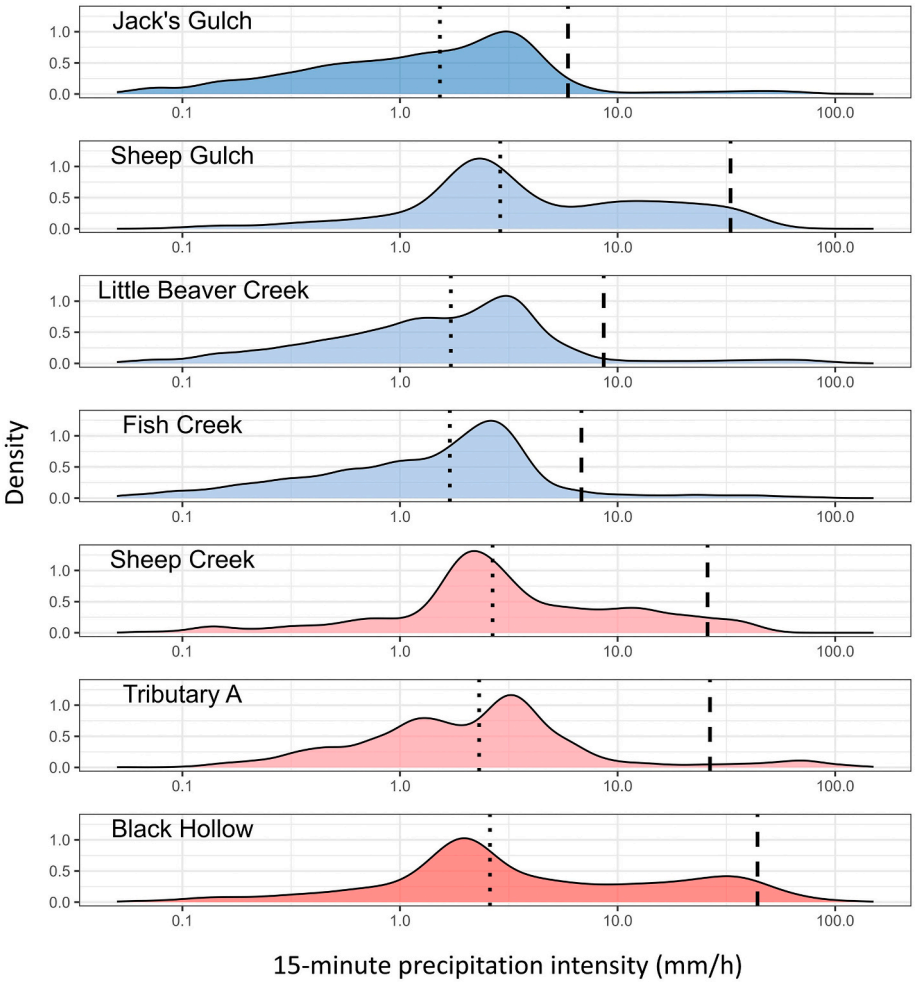

Fig. 4. Catchment-scale 15-min precipitation intensity density plots over the duration of each storm. The dotted line represents the median precipitation intensity at each catchment and the dashed line represents the 95th percentile precipitation intensity. The density plots are ordered and colored by the absorbing capacity ranking; dark blue is the catchment with the highest absorbing capacity and dark red is the catchment with lowest absorbing capacity.

Tributary A and Sheep Gulch ($p = 0.02$, $p = 0.0003$). Jack's Gulch has a lower mean of reach slopes than Little Beaver Creek Tributary A, Sheep Creek, and Sheep Gulch ($p = 0.0036$, $p = 0.0093$, $p < 0.001$). Little Beaver Creek has a lower reach slope mean than Little Beaver Creek Tributary A, Sheep Creek, and Sheep Gulch ($p < 0.0001$, $p < 0.001$, $p < 0.0001$).

The distribution of relative floodplain width among reaches varied between catchments ($p < 0.001$) (Fig. 6). The mean of the relative floodplain widths at Jack's Gulch is significantly greater than the relative floodplain widths at Sheep Gulch, Black Hollow, and Sheep Creek ($p < 0.001$, $p < 0.001$, $p = 0.02$). The mean of the relative floodplain widths at Little Beaver Creek is significantly greater than that of the relative floodplain widths at Black Hollow, Sheep Gulch, and Sheep Creek ($p < 0.001$, $p < 0.001$, $p = 0.003$). The mean of the relative floodplain widths is significantly greater at Fish Creek than at Sheep Gulch ($p = 0.02$). Jack's Gulch, Sheep Gulch, and Little Beaver Creek have 0.22, 0.43, and 0.17 km of reach stream length, respectively, that have a floodplain to channel width ratio >15. Jack's Gulch, Sheep Gulch, Little Beaver Creek, Fish Creek, and Little Beaver Creek Tributary A have 0.37, 0.43, 0.3, 0.46, and 0.8 km of stream length, respectively, with a floodplain to channel width ratio >10. There is a positive trend between floodplain to channel width ratio and response; catchments with greater absorption capacity are made up of reaches with greater floodplain to channel width ratios. The outlier to this trend is Sheep Gulch, which has the

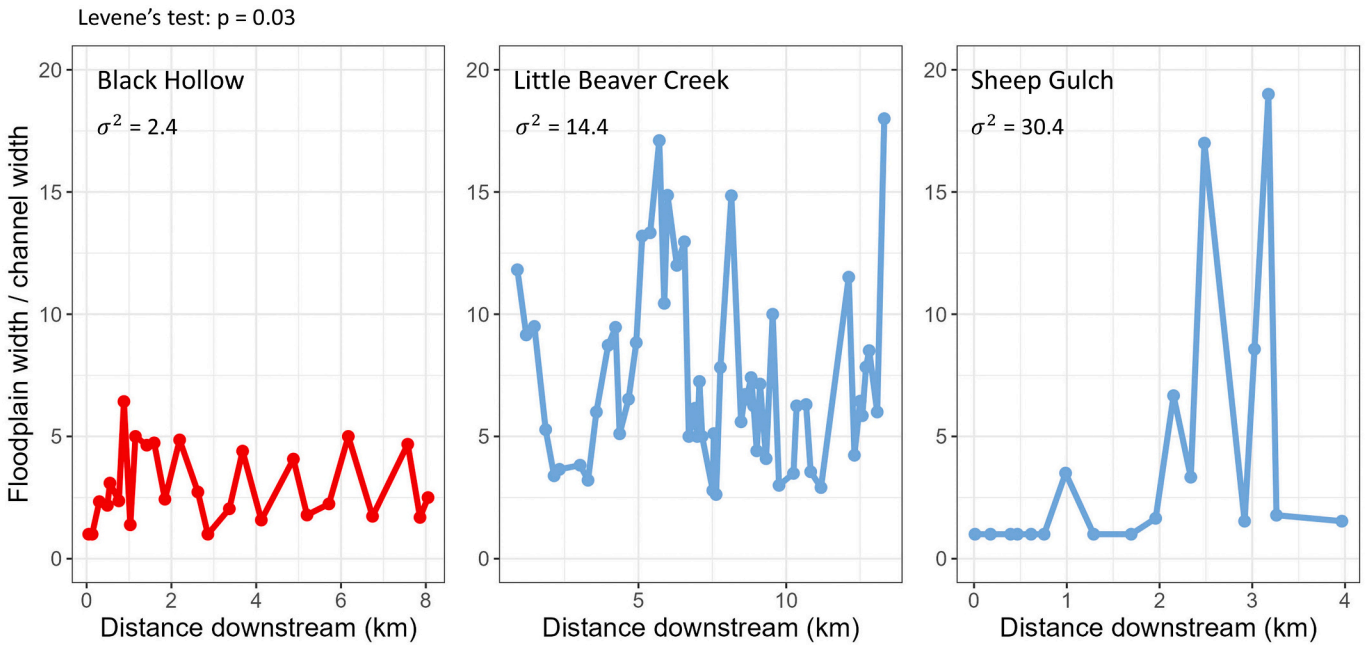

Fig. 5. Floodplain to channel width ratios plotted against distance downstream at Black Hollow, Little Beaver Creek, and Sheep Gulch. Black Hollow in red is an example of a catchment that did not absorb the impacts of disturbance. Little Beaver Creek and Sheep Gulch in blue are examples of catchments with different reach configurations that both absorbed the impacts of disturbance. Floodplain to channel width ratio variance (σ^2) differed between sites ($p < 0.03$). The variance of floodplain to channel width ratios at each site represents the inter-reach heterogeneity.

lowest mean floodplain to channel width ratio of all the sites while ranked as having only a large flood (Fig. 6a).

Beaver berms were present in at least one reach of every catchment except Sheep Creek (Fig. 7). Of the catchments with beaver berms present, the proportion of reaches with beaver berms ranged from 0.12 at Black Hollow to 0.38 at Fish Creek and Jack's Gulch. Beaver meadows were present in Little Beaver Creek, Sheep Gulch, and Jack's Gulch in 0.15, 0.06, and 0.31 of total reaches, respectively. The highest proportion of field-identified unburned reaches was at Little Beaver Creek at 0.26 followed by Sheep Gulch at 0.17 (Fig. 7). Sheep Creek, Fish Creek, and Black Hollow had the highest proportion of reaches burned at 0.90, 0.89, and 0.88, respectively. The median remotely sensed dNBR-derived burn extent of reaches was 100 % among all catchments except at Jack's Gulch, where the median burn extent was 0.72. Fish Creek had the highest proportion of reaches with willow present at 0.63 (Fig. 7). Black Hollow and Little Beaver Creek Tributary A had no reaches with willow present. Sheep Creek had aspen in 0.8 of reaches, the highest proportion among the study sites, but no willow.

The distribution of channel jam density values among reaches varied between catchments ($p < 0.001$) (Fig. 6). Fish Creek had greater mean channel jam density than Little Beaver Creek, Sheep Creek, and Black Hollow ($p = 0.009$, $p = 0.01$, $p = 0.01$, $p = 0.02$, Fig. 6). Sheep Gulch had greater mean channel jam density than Sheep Creek and Little Beaver Creek ($p = 0.03$, $p = 0.04$).

Of the six Poisson regression models tested using channel jams as the response variable, all models contained site as a predictor and bankfull channel area as an offset (Table 3). All models tested had reach slope, distance downstream, or both in the model. The top model had bankfull channel area as an offset with site, distance downstream, categorical floodplain vegetation, maximum channel count, bedform, and high burn severity related to the downstream spacing density of channel jams. This model describes a negative relationship between distance downstream and spatial density of channel jams among reaches in the study sites. This model indicates a higher spatial density of channel jam presence among reaches in each of the other study sites when compared to Black Hollow. The likelihood-ratio test (LRT) performed on this model indicates that there are significant differences between channel jams at different sites, distances downstream, with different floodplain vegetation, maximum channel counts, and proportions of high burn severity ($p < 0.001$ for all).

Floodplain jam density differed between sites ($p < 0.001$, Fig. 6). Jack's Gulch had lower floodplain jam density than Little Beaver Creek, Black Hollow, Fish Creek, and Sheep Gulch ($p < 0.001$, $p < 0.002$, $p < 0.001$, $p = 0.003$, Fig. 6). Of the six models tested with floodplain jams as the response variable, all models contained site and distance downstream as predictors and reach area as an offset (Table 3). The top model had reach area as an offset with site, distance downstream, high burn severity, and categorical floodplain vegetation as predictors. The LRT test on the model indicates that site, distance downstream, high burn severity, and categorical floodplain vegetation were related to the spatial density of floodplain jams ($p < 0.001$ for all). This model indicates a positive relationship between distance downstream and density of floodplain jam presence among reaches in the study sites. This model also indicates a lower rate of floodplain jam presence among reaches in each of the study sites, apart from Sheep Gulch, when compared to Black Hollow.

4.4. Sensitivity analysis

A paired *t*-test shows that the field-measured bankfull channel widths increased between 2018 and 2023 ($p = 0.002$) and the associated floodplain widths did not change between the years of this study at Little Beaver Creek. At Black Hollow, the channel widths measured using field and remote methods did not statistically differ despite the observed changes to form, but the floodplain widths measured in the field were different than the valley widths measured using the pre-event DEM ($p = 0.03$).

5. Discussion

Our field-based criteria for ranking catchments with respect to absorbing capacity were chosen based on lack of direct measurements of sediment export during disturbances from individual catchments and the predominance of coarse-sediment export during floods and debris

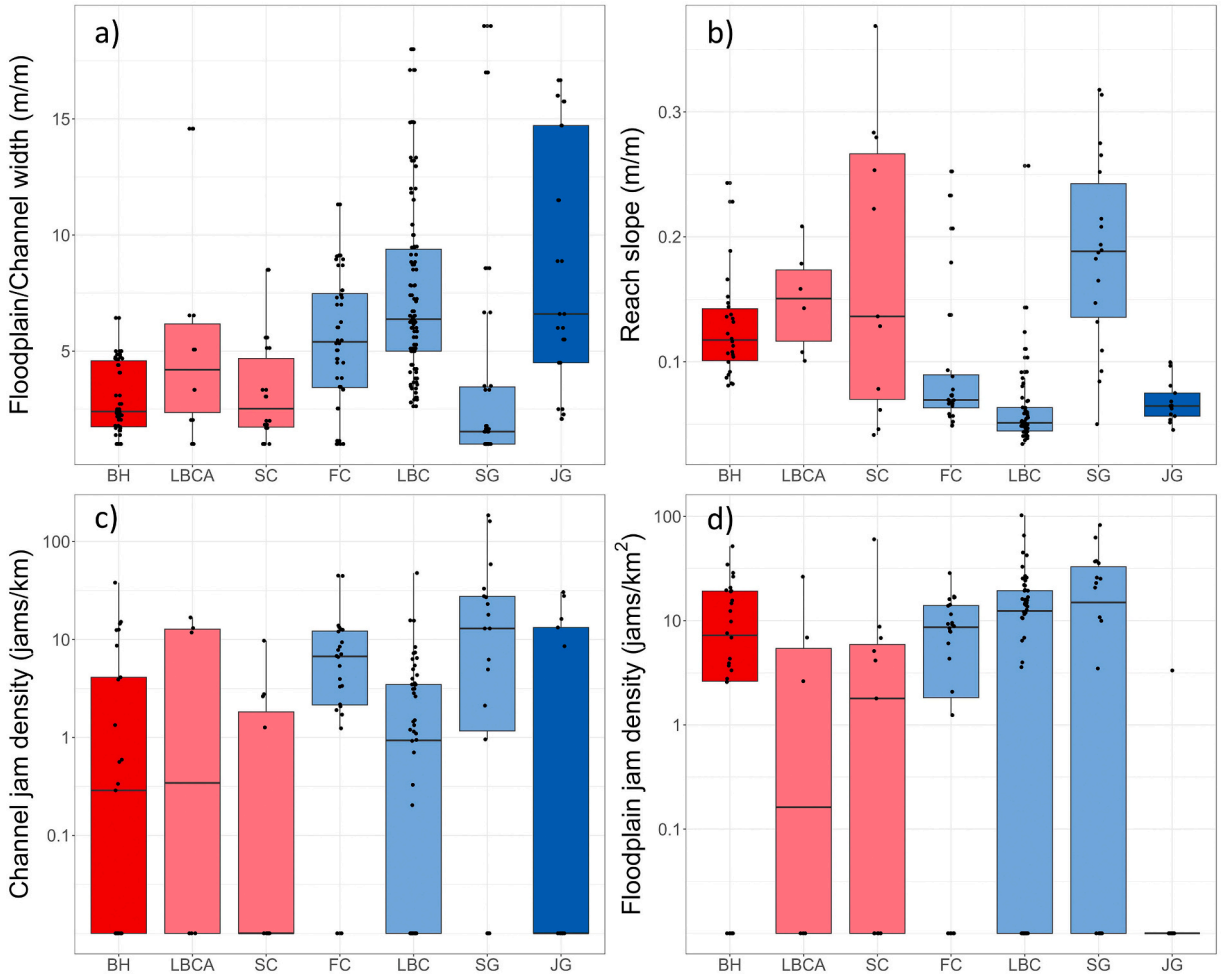

Fig. 6. Interquartile distributions of reach characteristics at each site with the site that absorbed disturbance the least in dark red on the left (BH) and the most in dark blue on the right (JG). a) Floodplain to channel width ratio varied between catchments ($p < 0.001$). b) Reach slope varied between catchments ($p < 0.001$). c) Channel logjam density distribution varied between catchments ($p < 0.001$). d) Floodplain logjam density distribution varied between catchments ($p < 0.001$).

flows in this study area. These criteria may be suitable for other regions, but we recommend that investigators working elsewhere develop site-specific but analogous criteria for absorbing capacity based on regional characteristics and available information.

5.1. Sensitivity analysis

Reach-scale geomorphic characteristics were all measured post-event. These measurements therefore reflect the state of the river corridor after the impacts of fire and flood have been absorbed or caused a shift to another state. Because we measured bankfull channel widths based on evidence of the most recent peak snowmelt flow, the field-measured channel widths measured at Black Hollow in 2023 are likely representative of pre-event channel geometry. This is supported by the comparison of field-measured data post-event and remotely measured data pre-event. Although the field-measured channel widths post-flood at Black Hollow do not differ from the pre-flood remote measurements, the geometry of the channel undoubtedly changed during the flood.

5.2. Hydroclimatic flooding thresholds

Although most of the catchment areas are above the 2300 m elevation limit for rainfall flooding in Colorado (Jarrett, 1990), we observed flooding caused by summer convective storms in these catchments following the Cameron Peak fire (Fig. 8). Under normal conditions, rainfall intensity would not be sufficient to cause flooding of the magnitude observed and flood peaks would typically be caused by snowmelt. Post-fire, every event we observed was caused by rainfall during summer convective storms. Because water is more efficiently conveyed from hillslope to channel on a burned landscape, rainfall causes disproportionate flooding compared to unburned landscapes (Moody and Martin, 2001). On a burned landscape, the removal of organic material as groundcover and associated increases in runoff and erosion relative to rainfall seem to be manifesting as a shift in the elevation above which storms cause rainfall-induced flooding at these sites. In the context of these study sites, this could be conceptualized as fire influencing the elevation threshold below which rainfall-induced flooding occurs in the Front Range. This corresponds to observed upslope migration of channel heads following wildfire in the region (Wohl, 2013).

5.3. Characteristics associated with capacity to absorb disturbance

The first hypothesis, that lesser response to disturbance will correspond to more resisting and fewer driving characteristics at the catchment scale, was partially supported. We saw that individual geomorphic and burn characteristics were not associated with response to disturbance. Precipitation was a characteristic that drove response to disturbance, which aligns with the metrics proposed by recent debris flow models (Gartner et al., 2014; Staley et al., 2017). Other studies have found that catchment morphology and lithology correlate with post-fire

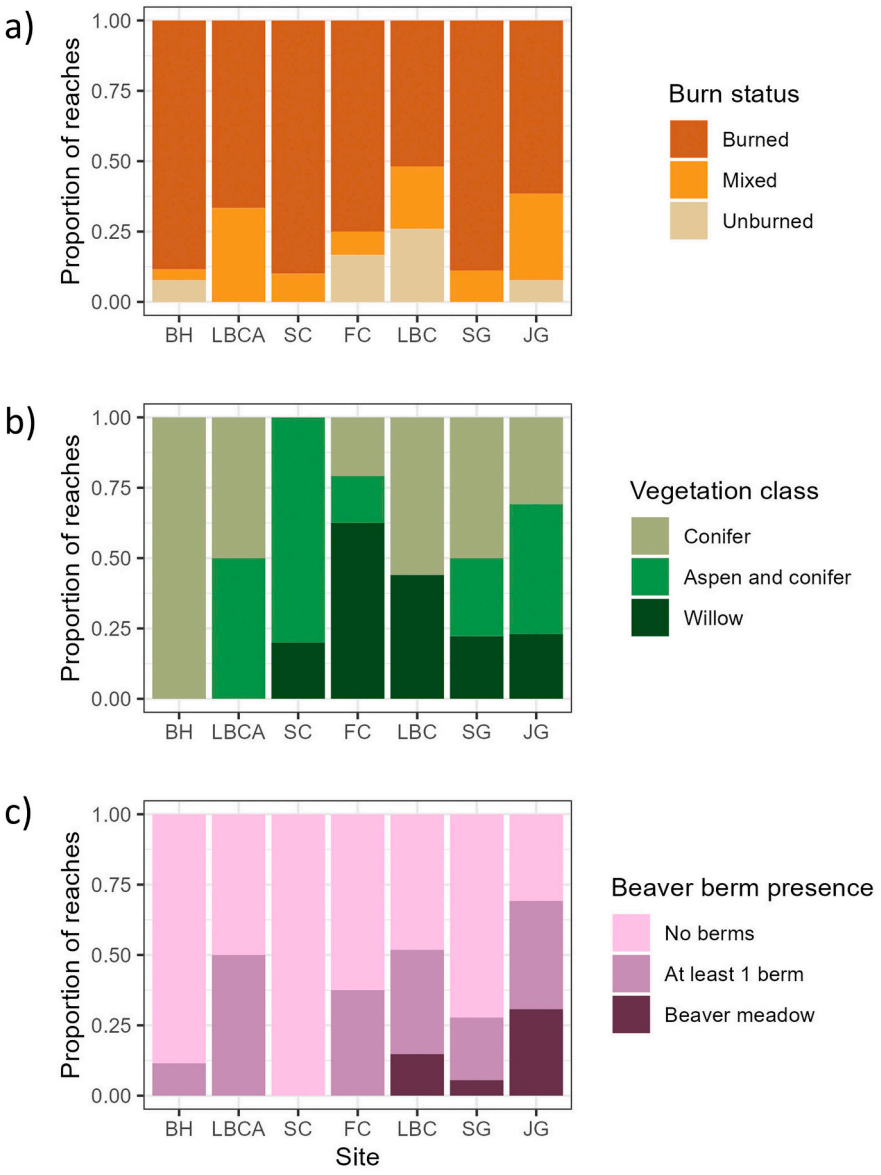

Fig. 7. Stacked bar plot with the proportion of reaches in different classes at each site. a) Proportion of reaches in each burn category where dark orange bars represent burned reaches, light orange bars represent reaches with mixed burn, and tan bars represent unburned reaches. b) Proportion of reaches in each vegetation category where light green bars represent reaches with only conifers present, medium green bars represent reaches where aspen and conifers were present, and dark green bars represent reaches where willow were present. c) Proportion of reaches with different levels of beaver modified topography where pink bars represent reaches with no beaver berms, light purple bars represent reaches with at least one beaver berm, and dark purple bars represent reaches that were dominated by beaver modified topography, or a beaver meadow.

debris flow occurrence (Menitove, 1999; Cannon and Reneau, 2000), but these characteristics did not explain the trends in catchment response within the scope of this project. The study catchments had many large-scale characteristics in common due to their physical proximity to each other, including lithology, soil type, and burn characteristics (Triantafillou, 2024), but the catchments represent a range of sizes and mean slopes for headwater catchments.

We found no trend between the response and catchment area or mean basin slope, a conclusion that is supported by some but not all previous studies (Pelletier and Orem, 2014; Wagenbrenner and Robichaud, 2014). Cannon and Reneau (2000) found that of three catchments with a range of responses after fire, a debris flow was generated at the catchment with the steepest hillslopes. Contrasting these findings, in a study of 95 burned catchments across fire-prone regions of North America, the catchments that produced debris flows could not be distinguished from those that did not produce debris flows by catchment area and slope (Cannon, 2001). Debris flow prediction models also take slope into account in at least one form (Gartner et al., 2014; Staley et al., 2017). The mean catchment slope calculated in this study is for the entire basin, not just the river corridor. Based on field observations, sediment was derived from the river corridor, highlighting the importance of spatial scale and valley bottom geometry. The negative relationship between response and precipitation intensity indicates that precipitation was driving response to disturbance. Although there was a relationship between response and precipitation, there was a range of precipitation intensities within response categories, indicating that precipitation is one of many characteristics influencing response.

As catchment-scale characteristics do not completely explain the range of responses to disturbance, we next look to reach-scale characteristics. Reach characteristics that were conceptualized as resisting response to disturbance, including inter- and intra-reach heterogeneity elements, were associated with greater absorption capacity, supporting

Table 3
The Poisson models tested to describe channel and floodplain jams as the outcome. The AIC and delta AIC relative to the best model were used to select the best models to describe each jam type. The models and associated metrics in bold were selected as the best performing models. Delta AIC values closer to zero indicate models that perform nearly as well as the best model.

Outcome	Model	Predictors	AIC	Delta AIC
Channel jams	1	Site + offset(log(channel area)) + distance downstream	1013.3	156.5
Channel jams	2	Site + offset(log(channel area)) + reach slope	1101.9	245.1
Channel jams	3	Site + offset(log(channel area)) + reach slope + distance downstream + floodplain vegetation + maximum channel count + bedform	907.2	50.4
Channel jams	4	Site + offset(log(channel area)) + distance downstream + floodplain vegetation + maximum channel count + bedform + burn severity high	901.2	44.4
Channel jams	**5**	**Site + offset(log(channel area)) + distance downstream + floodplain vegetation + maximum channel count + bedform + burn severity high**	**856.8**	**0**
Channel jams	6	Site + offset(log(channel area)) + reach slope + distance downstream + maximum channel count + bedform + burn severity high	908.7	51.9

Floodplain jams	Model	Predictors	AIC	Delta AIC
Floodplain jams	1	Site + offset(log(reach area)) + distance downstream	2069.5	304.4
Floodplain jams	2	Site + offset(log(reach area)) + distance downstream + burn severity high	2061.5	296.4
Floodplain jams	3	Site + offset(log(reach area)) + distance downstream + burn severity high + basal area	2002.2	237.1
Floodplain jams	**4**	**Site + offset(log(reach area)) + distance downstream + burn severity high + floodplain vegetation**	**1765.1**	**0**
Floodplain jams	5	Site + offset(log(reach area)) + distance downstream + burn severity high + maximum channel count + floodplain vegetation	1767.1	2
Floodplain jams	6	Site + offset(log(reach area)) + distance downstream + burn severity high + maximum channel count + floodplain vegetation + basal area	1769.0	3.9

hypotheses 2 (greater inter-reach heterogeneity corresponds to lesser response to disturbance) and 3 (greater resisting and fewer driving characteristics at the reach scale correspond to lesser response). Reach-scale slope and burn extent, conceptualized as driving response to disturbance, were associated with less capacity to absorb disturbance. This aligns with other studies in which the average channel gradient within a catchment was a key parameter in debris flow generation in burned catchments (Cannon and Reneau, 2000). Compared to the burn characteristics on the catchment-scale that were not associated with response to disturbance, these results on the reach scale indicate that the impacts of fire on the river corridor have a disproportionate effect on the post-fire response relative to the impacts of fire on the hillslope. More resilient catchments had greater inter-reach scale heterogeneity, more reaches with wide floodplains, lower channel gradients, multiple channels, beaver-modified topography, and multi-stem deciduous vegetation including willow, supporting hypotheses 2 and 3.

There were significantly different floodplain and channel jam densities among the study catchments, indicating different responses to flooding. The negative trend between distance downstream and channel jams and the positive relationship between distance downstream and floodplain jams indicates a transition from transport-limited to supply-limited from headwaters to outlet (Marcus et al., 2002). Focusing on channel jams, the transport-limited reaches occur at the upstream-most headwaters where there is capacity for wood recruitment from the banks, but there is low capacity to move this wood into a jam. Moving downstream, the transport capacity increases and is balanced with the supply capacity. This is where the maximum channel jam densities are expected. As the wood-transport capacity increases downstream with increasing contributing drainage area and becomes greater than the wood-supply capacity, we observed decreasing jam density at the downstream end of the catchment. The longitudinal trends we described in channel jam density align with previous studies (Wohl and Jaeger, 2009). The positive relationship between distance downstream and floodplain jam density indicates that the downstream limit of the system that we observed only captured the transport-limited and maximum jam portions of the catchment. It is likely that the fire and flood disturbances shifted the distribution of channel and floodplain jams with respect to locations for transport- and supply-limited thresholds of logjams (Wohl et al., 2024a).

The reach-scale ratio of the floodplain to channel width was hypothesized as a resisting characteristic to disturbance response. The floodplain to channel width ratios were greater at the sites that were ranked as having more absorbing capacity compared to the three catchments that had low absorbing capacity, except for Sheep Gulch. At Little Beaver Creek, a site representing a greater absorbing capacity, the distribution of the floodplain to channel ratios was high because there were many reaches with wide floodplains. Once accessed during a flood, floodplains that are longer, wider, and have more hydraulic roughness increase attenuation of peak discharge and dissipate energy during floods by slowing flows (O'Sullivan et al., 2012; Lininger and Latrubesse, 2016). Valley characteristics including floodplain size, stream gradient, and roughness influence peak discharge and can substantially moderate floods (Woltemade and Potter, 1994), as we quantified at the study sites.

5.4. *The importance of longitudinal and temporal sequencing*

Among many characteristics on the reach scale, Sheep Gulch did not align with many of the trends observed. Although it was ranked as having only a large flood, many parameters aligned more closely to those measured at Sheep Creek to which it is a tributary almost equal in size. In the upper catchment, there Sheep Gulch and Sheep Creek had many characteristics in common on the reach scale. There were patterns of erosion and deposition within the channel that showed evidence of a large flood in both catchments with erosion and evidence of flood magnitude growing with a downstream progression (Fig. 9). In Sheep Creek, this pattern continued to the outlet of the catchment where the channel shifted and incised, and then deposited a sediment fan. In Sheep Gulch, the patten of erosion and deposition related to the flood continued throughout the upper two-thirds of the catchment. At this point in the catchment, a series of reaches that were wider, lower gradient, and less incised included evidence of relict beaver dams, willow, and aspen recovering from the fire. The floodplain was wet during the time of data collection at the end of July, indicating a well-connected channel and floodplain (Fig. 9). Below the wide reaches, there was no evidence of the major flood that had been bulking up as it moved downstream in the upper part of the catchment. In other words, the wide and hydraulically rough reaches at the downstream end of Sheep Gulch appear to have effectively attenuated the water and sediment fluxes coming downstream, absorbing the impacts of disturbance and therefore promoting catchment-scale resilience.

Although not the focus of this study, the time between the fire and subsequent storms likely affects the magnitude of response. The changes that influence the production of runoff and sediment diminish as the

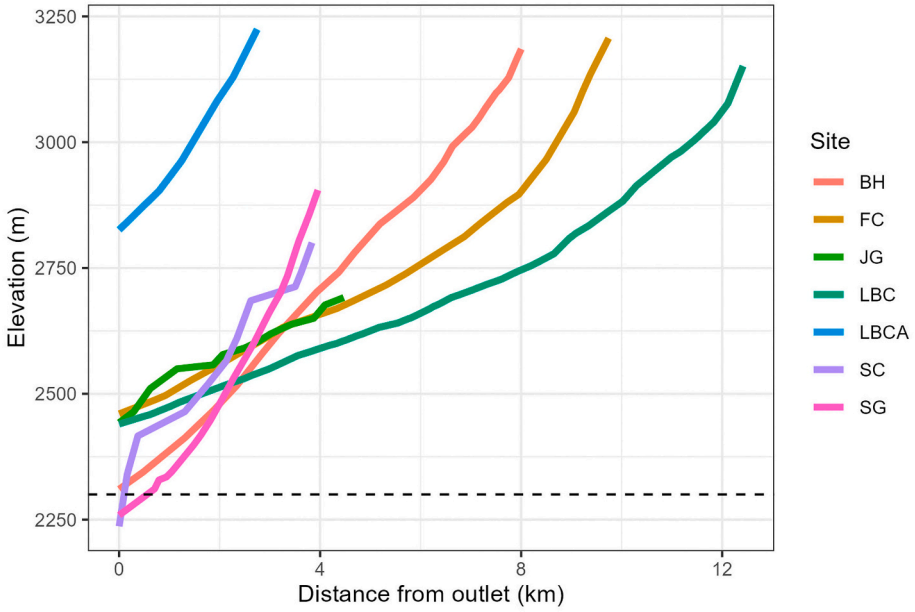

Fig. 8. Elevation profiles of each of the study catchments in solid lines. The dashed horizontal line at 2300 m represents the elevation threshold above which floods in Colorado are typically caused by snowmelt instead of rainfall (Jarrett, 1990). Flooding at elevations above this threshold is typically produced by snowmelt.

Fig. 9. Sheep Gulch river corridor downstream progression. a) Upper Sheep Gulch with a confined channel and no floodplain. Dashed yellow lines outline the river corridor. b) Channel and bank scouring in Sheep Gulch in the upper part of the catchment. c) Wide floodplain in the lower part of the Sheep Gulch catchment. Dashed yellow lines outline the floodplain with a yellow box around a person for scale. d) A reach below the wide floodplain reach. There is less incision and erosion of banks.

landscape recovers from the impacts of fire over time. Vegetation regrowth decreases sediment production from hillslopes and river corridor. Additionally, the sediment supply in low-order tributaries is exhausted and the system becomes supply-limited.

5.5. Geomorphic changes

The assumption underpinning our observations is that the floods that caused geomorphic change at these sites activated the entire floodplain. Depending on the response of a site, the change in floodplain form may affect future floodplain function. At Black Hollow, the river incised to such a degree that even an event of the same magnitude would likely no longer activate the floodplain that we identified in the field. This will likely act as a terrace or very disconnected floodplain. Thus, the form and function of the river corridor have changed, creating a different state. At Little Beaver Creek, a more resilient site, the floodplain identified in the field likely remains a functioning, connected floodplain in many reaches. Although the channel incised in some reaches, there are many reaches within the catchment that did not change in this way. This river corridor absorbed the impacts of the flood disturbance and maintained the ability to perform the same function. Although there was geomorphic change within this river corridor in the form of channel widening, these changes did not fundamentally alter river corridor forms and processes. For example, the multithread reaches changed their primary flow path but remained multithread. The floodplains in some locations were reconfigured with the deposition of imbricated boulders and the formation of secondary floodplain channels, but floodplain function in attenuating flows remained the same, perhaps enhanced by the heterogeneity elements.

Spatial heterogeneity creates a positive feedback that increases in response to disturbance. Studies have shown that spatial heterogeneity in the form of beaver-modified topography, sediment, and logjams create more heterogeneity in reaches with wide floodplains (Czuba and Foufoula-Georgiou, 2015; Wohl et al., 2022; Wohl et al., 2024a). In the context of these sites, beaver berms trap wood and create logjams. At Little Beaver Creek, the in-channel jams perpetuated spatial heterogeneity by creating obstructions and supplying wood, facilitating formation of floodplain jams. These floodplain jams created more spatial heterogeneity by creating secondary channels and will likely increase the capacity to absorb the impacts of disturbance by attenuating flows that access the floodplain. In Black Hollow, where the floodplains will likely not be accessed, the floodplain jams may still be enhancing absorption by attenuating flows from the unvegetated hillslopes. These cycles of self-enhancing heterogeneity illustrate resilient systems undergoing change to absorb the impacts of disturbance and reinforce the processes occurring to hold the system in a stable dynamic state, increasing the resilience to disturbance.

5.6. Management significance and resilience implications

Post-fire impacts to rivers can be harmful to human communities and resources. Increased sediment levels entering drinking water treatment facilities reduce the rates of water processing (Smith et al., 2011; Bladon et al., 2014; Gannon et al., 2021). River restoration resulting in channel reconfiguration can increase the attenuation of flood pulses (Sholtes and Doyle, 2011). The research presented here suggests that restoration efforts aiming to increase absorbing capacity may be most effective when focused on a small spatial scale, defined as a reach in this study. Restoration efforts aimed at increasing resilience to disturbance in the river corridor should focus on increasing the absorbing capacity through spatial heterogeneity within and between reaches.

Catchments that exhibited greater absorbing capacity in this study had more reaches with a capacity for attenuation, so reach-scale projects that focus on connecting the channel and floodplain where a wider valley floor is naturally present are likely an effective strategy. Sheep Gulch illustrated how the post-fire catchment response can be impacted by a small number of reaches with a capacity for attenuation lower in the catchment, further supporting and informing future restoration efforts directed at the scale of individual reaches to address whole-catchment response to wildfire.

6. Conclusions

The role of river corridor form and process in promoting landscape resilience after wildfire is becoming a focus of research and management. In this study, we assessed the impacts of characteristics at the catchment and reach scales on the resilience response after wildfire by ranking each of seven catchments on a scale of relative absorbing capacity based on the geomorphic evidence of sediment export. Results presented here indicate that absorbing capacity was most closely related to characteristics on the reach-scale. Of the catchment characteristics assessed, greater absorbing capacity was associated with lower precipitation intensity. Greater absorbing capacity was associated with catchments made up of more reaches with wide floodplains, low channel gradient, multiple channels, beaver-modified topography, and multistem deciduous vegetation.

One catchment was ranked as having greater absorbing capacity compared to many other catchments, but it had high precipitation intensity and reach slope, characteristics that aligned with the less absorbent catchments. Although there was evidence of flooding and significant incision throughout much of the river corridor, a series of three wide reaches in the lower two-thirds of the catchment apparently attenuated the flood flows. These results suggest that resilient catchments may not need to have the capacity for attenuation and disturbance absorption evenly distributed throughout the river corridor. Additionally, multiple reaches with attenuation in succession may provide redundancy and attenuate flood flows even after floods increase in magnitude downstream. Therefore, while many reaches with a capacity for attenuation create a resilient catchment, there are different configurations of reaches that make up river corridors with enhanced resilience.

Funding

U.S. Geological Survey 104b grant FY2023.

CRediT authorship contribution statement

Shayla Triantafillou: Writing – review & editing, Writing – original draft, Visualization, Methodology, Investigation, Formal analysis, Conceptualization. **Ellen Wohl:** Writing – review & editing, Methodology, Investigation, Funding acquisition, Conceptualization.

Declaration of competing interest

The authors declare that they have no known competing financial interests or personal relationships that could have appeared to influence the work reported in this paper.

Data availability

Data are available at https://doi.org/10.5061/dryad.qfttdz0r3

Acknowledgements

We thank Sarah Dunn, Madeline Ferguson, Claire Pickerel, Maya Daurio, Connor Mertz, Brady Jones, for assistance in the field and Francis Rengers, Phoebe White, Megan Sears, Kayleigh Keller, and Ann Hess for support with analyses. This manuscript benefited from the input of three anonymous reviewers.

Appendix A. Supplementary Information

Supplementary information for this article can be found online at https://doi.org/10.1016/j.geomorph.2024.109446.

References

Abatzoglou, J.T., Kolden, C.A., Williams, A.P., Lutz, J.A., Smith, A.M.S., 2017. Climatic influences on interannual variability in regional burn severity across western US forests. Int. J. Wildland Fire 26 (4), 269. https://doi.org/10.1071/WF16165.

Abatzoglou, J.T., Williams, A.P., 2016. Impact of anthropogenic climate change on wildfire across western US forests. Proc. Natl. Acad. Sci. 113 (42), 11770–11775. https://doi.org/10.1073/pnas.1607171113.

Abatzoglou, J.T., Williams, A.P., Boschetti, L., Zubkova, M., Kolden, C.A., 2018. Global patterns of interannual climate–fire relationships. Glob. Chang. Biol. 24 (11). https://doi.org/10.1111/gcb.14405. Article 11.

Ader, E., Wohl, E., McFadden, S., Singha, K., 2021. Logjams as a driver of transient storage in a mountain stream. https://onlinelibrary.wiley.com/doi/full/10.1002/esp.5057.

Alessio, P., Dunne, T., Morell, K., 2021. Post-Wildfire Generation of Debris-Flow Slurry by Rill Erosion on Colluvial Hillslopes. J. Geophys. Res. Earth 126 (11), e2021JF006108. https://doi.org/10.1029/2021JF006108.

Battige, K., 2022. Fish Survey and Management Information. Colorado Parks and Wildlife.

Benavides-Solorio, J., MacDonald, L.H., 2001. Post-fire runoff and erosion from simulated rainfall on small plots. Colorado Front Range. Hydrological Processes 15 (15), 2931–2952. https://doi.org/10.1002/hyp.383.

Bladon, K.D., Emelko, M.B., Silins, U., Stone, M., 2014. Wildfire and the Future of Water Supply. Environ. Sci. Technol. 48(16), Article 16, 130g. https://doi.org/10.1021/es500.

Blount, K., Ruybal, C.J., Franz, K.J., Hogue, T.S., 2020. Increased water yield and altered water partitioning follow wildfire in a forested catchment in the western United States. Ecohydrology 13 (1). https://doi.org/10.1002/eco.2170. Article 1.

Bowman, D.M.J.S., Balch, J.K., Artaxo, P., Bond, W.J., Carlson, J.M., Cochrane, M.A., D'Antonio, C.M., DeFries, R.S., Doyle, J.C., Harrison, S.P., Johnston, F.H., Keeley, J. E., Krawchuk, M.A., Kull, C.A., Marston, J.B., Moritz, M.A., Prentice, I.C., Roos, C.I., Scott, A.C., Pyne, S.J., 2009. Fire in the Earth System. Science 324 (5926), 481–484. https://doi.org/10.1126/science.1163886.

Burchsted, D., Daniels, M., Thorson, R., Vokoun, J., 2010. The River Discontinuum: Applying Beaver Modifications to Baseline Conditions for Restoration of Forested Headwaters. BioScience 60 (11), 908–922. https://doi.org/10.1525/bio.2010.60.11.7.

Cannon, S.H., 2001. Debris-flow generation from recently burned watersheds. Environ. Eng. Geosci. 7 (4), 321–341. https://doi.org/10.2113/gseegeosci.7.4.321.

Cannon, S.H., Gartner, J.E., 2005. Wildfire-related debris fow from a hazards perspective. In: Chapter 15 in: Jakob, M. and Hungr, O. (Ed.), Debris Flow Hazards and Related Phenomena. Praxis, Springer, Berlin, Heidelberg, pp. 363–385. https://doi.org/10.1007/3-540-27129-5_15.

Cannon, S.H., Gartner, J.E., Wilson, R.C., Bowers, J.C., Laber, J.L., 2008. Storm rainfall conditions for floods and debris flows from recently burned areas in southwestern Colorado and southern California. Geomorphology 96 (3–4), 250–269. https://doi.org/10.1016/j. geomorph.2007.03.019.

Cannon, S.H., Reneau, S.L., 2000. Conditions for generation of fire-related debris flows, Capulin Canyon, New Mexico. Earth Surf. Process. Landf. 25 (10), 1103–1121. https://doi.org/10.1002/1096-9837(200009)25:10<1103::AID-ESP120>3.0.CO;2-H.

National Interagency Fire Center, 2022. Inter Agency Fire Perimeter history. https://data-nifc.opendata.arcgis.com/datasets/e02b85c0ea784ce7bd8add7ae3d293d0_0/explore.

Chapman, S.S., Griffith, G.E., Omernik, J.M., Price, A.B., Freeof, J., Schrupp, D.L., 2006. Ecoregions of Colorado: U.S. Geological Survey Level IV Ecoregions 2 sided color poster with map, descriptive text, summary tables, and photographs. http://www.cologicalregions.info/data/co/co_front.pdf.

Collins, B.D., Montgomery, D.R., Fetherston, K.L., Abbe, T.B., 2012. The floodplain large-wood cycle hypothesis: a mechanism for the physical and biotic structuring of temperate forested alluvial valleys in the North Pacific coastal ecoregion. Geomorphology 139–140, 460–470. https://doi.org/10.1016/j.geomorph.2011.11.011.

Corenblit, D., Steiger, J., Dufour, S., Liébault, F., Piégay, H., 2024. Resilience and the biophysical science of rivers. In: Resilience and Riverine Landscapes. Elsevier, pp. 269–286. https://doi.org/10.1016/B978-0-323-91716-2.00010-8.

Czuba, J.A., Foufoula-Georgiou, E., 2015. Dynamic connectivity in a fluvial network for identifying hotspots of geomorphic change. Water Resour. Res. 51 (3), 1401–1421. https://doi.org/10.1002/2014WR016139.

Davis, W.M., 1898. The grading of mountain slope. Science 7 (81).

DeBano, L.F., 2000. The role of fire and soil heating on water repellency in wildland environ- ments: a review. J. Hydrol. 231–232, 195–206. https://doi.org/10.1016/S0022-1694(00) 00194-3.

Dennison, P.E., Brewer, S.C., Arnold, J.D., Moritz, M.A., 2014. Large wildfire trends in the western United States, 1984–2011. Geophys. Res. Lett. 41 (8). https://doi.org/10.1002/2014GL059576. Article 8.

DiBiase, R.A., Lamb, M.P., 2020. Dry sediment loading of headwater channels fuels post-wildfire debris flows in bedrock landscapes. Geology 48, 189–193.

Downing, J., 2012. Global abundance and size distribution of streams and rivers. Inland Waters 2 (4), 229–236. https://doi.org/10.5268/IW-2.4.502.

Dunn, O.J., 1964. Multiple comparisons using rank sums. Technometrics 6, 241–252.

Dunn, S.B., 2023. *Dammed Ponds! A Study of Post-Fire Sediment and Carbon Dynamics in Beaver Ponds and their Contributions to Watershed Resilience* [M.S.]. Colorado State University.

Dunn, S.B., Rathburn, S.L., Wohl, E., 2024. Post-fire sediment attenuation in beaver ponds, Rocky Mountains, CO and WY, USA. Earth Surf. Process. Landf. esp.59, 70. https://doi.org/10.1002/esp.5970.

Entwistle, N., Heritage, G., Milan, D., 2018. Flood energy dissipation in anabranching channels: Flood energy dissipation in anabranching channels. River Res. Appl. 34 (7), 709–720. https://doi.org/10.1002/rra.3299.

Fairfax, E., Whittle, A., 2020. Smokey the Beaver: Beaver-dammed riparian corridors stay green during wildfire throughout the western United States. Ecol. Appl. 30 (8), e02225. https://doi.org/10.1002/eap.2225.

Fox, J., Weisberg, S., 2019. *An R Companion to Applied Regression* (Version 3) [R]. https://socialsciences.mcmaster.ca/jfox/Books/Companion/.

Fuller, I.C., Gilvear, D.J., Thoms, M.C., Death, R.G., 2019. Framing resilience for river geomorphology: Reinventing the wheel?: Framing resilience for river geomorphology. River Res. Appl. 35 (2), 91–106. https://doi.org/10.1002/rra.3384.

Gannon, B.M., Wei, Y., Thompson, M.P., Scott, J.H., Short, K.C., 2021. System analysis of wildfire-water supply risk in colorado, usa with monte carlo wildfire and rainfall simulation. Risk Analysis. https://doi.org/10.1111/risa.13762.

Gartner, J.E., Cannon, S.H., Santi, P.M., 2014. Empirical models for predicting volumes of sediment deposited by debris flows and sediment-laden floods in the transverse ranges of southern California. Eng. Geol. 176, 45–56. https://doi.org/10.1016/j.enggeo.2014.04. 008.

Graham, R.T., 2003. *Hayman Fire Case Study* RMRS-GTR-114; P. In: RMRS-GTR-114. U.S. Department of Agriculture, Forest Service, Rocky Mountain Research Station. https://doi.org/10.2737/RMRS-GTR-114.

Green, G.N., 1992. *The Digital Geologic Map of Colorado in ARC/INFO Format* (92–507-D-O; Open-File Report). U.S, Geological Survey.

Grimm, M.M., Wohl, E.E., Jarrett, R.D., 1995. Coarse-sediment distribution as evidence of an elevation limit for flash flooding, Bear Creek. Colorado. Geomorphology 14 (3), 199–210. https://doi.org/10.1016/0169-555X(95)00037-6.

Hansen, W.R., Chronic, J., Matelock, J., 1978. Climatography of the front range urban corridor and vicinity, Colorado. Geol. Surv. Prof. Pap. 1019, 1019.

Horton, J.D., 2017. *The State Geologic Map Compilation (SGMC) Geodatabase of the Conterminous United States* [Dataset]. https://doi.org/10.5066/F7WH2N65.

Horton, R.E., 1932. Drainage-basin characteristics. EOS Trans. Am. Geophys. Union 13 (1), 350–361. https://doi.org/10.1029/TR013i001p00350.

Engineering Center Hydrologic, USACE, 2023. Basin Characteristic. In: HEC-HMS Users Manual, pp. 222–226. https://www.hec.usace.army.mil/confluence/hmsdocs/hmsum/4.8/geographic-information/basin-characteristics.

Hynes, H.B.N., 1975. The stream and its valley. Verb. Internat. Verein. Limnol. 19, 1–15.

Jarrett, R.D., 1990. Paleohydrologic techniques used to define the spatial occurrence of floods. Geomorphology 3 (2), 181–195. https://doi.org/10.1016/0169-555X(90)90044-Q.

Jarrett, R.D., 1993. Flood Elevation Limits in the Rocky Mountains. American Society of Civil Engineers.

Jones, J.B., Smock, L.A., 1991. Transport and retention of particulate organic matter in two low-gradient headwater streams. J. N. Am. Benthol. Soc. 10 (2), 115–126. https://doi.org/10.2307/1467572.

Kostelnik, J., Schmitt, R.G., Rengers, F.K., Kean, J.W., 2022. *Cameron Peak Fire: Flooding and Debris Flows* [Story Map]. https://landslides.usgs.gov/storymap/cameronpeak/.

Lenth, R.V., 2023. *Emmeans: estimated marginal Means, aka Least-Squares Means* (1.8.8) [R]. https://CRAN.R-project.org/package=emmeans.

Lininger, K.B., Latrubesse, E.M., 2016. Flooding hydrology and peak discharge attenuation along the middle Araguaia River in Central Brazil. CATENA 143, 90–101. https://doi.org/10.1016/j. catena.2016.03.043.

Livers, B., Wohl, E., 2016. Sources and interpretation of channel complexity in forested subalpine streams of the Southern Rocky Mountains. Water Resour. Res. 52 (5), 3910–3929. https://doi.org/10.1002/2015WR018306.

Madole, R.F., VanSistine, D.P., Michael, J.A., 1998. Pleistocene Glaciation in the Upper Platte River Drainage Basin. IMAP, Colorado. https://doi.org/10.3133/i2644.

Malone, D., Rondeau, R., & Decker, K. (2019). *Rocky Mountain Subalpine-Montane Riparian Shrubland: Colorado Natural Heritage Program*. https://cnhp.colostate.edu/projects/ ecological-systems-ofcolorado/.

Marcus, W.A., Marston, R.A., Colvard, C.R., Gray, R.D., 2002. Mapping the spatial and temporal distributions of woody debris in streams of the Greater Yellowstone Ecosystem, USA. Geomorphology 44 (3–4), 323–335. https://doi.org/10.1016/S0169-555X(01) 00181-7.

Marshall, A., Iskin, E., Wohl, E., 2021. Seasonal and diurnal fluctuations of coarse particulate organic matter transport in a snowmelt-dominated stream. River Res. Appl. 37 (6), 815–825. https://doi.org/10.1002/rra.3802.

Martin, D.A., Moody, J.A., 2001. Comparison of soil infiltration rates in burned and unburned mountainous watersheds. Hydrol. Process. 15 (15). https://doi.org/10.1002/hyp.380. Article 15.

Mast, M.A., Clow, D.W., 2008. Effects of 2003 wildfires on stream chemistry in Glacier National Park. Montana. Hydrological Processes 22 (26), 5013–5023. https://doi.org/10.1002/hyp.7121.

McGuire, L.A., Youberg, A.M., 2019. Impacts of successive wildfire on soil hydraulic properties: Implications for debris flow hazards and system resilience. Earth Surf. Process. Landf. 44 (11). https://doi.org/10.1002/esp.4632. Article 11.

McGuire, L.A., Youberg, A.M., Rengers, F.K., Abramson, N.S., Ganesh, I., Gorr, A.N., Hoch, O., Johnson, J.C., Lamom, P., Prescott, A.B., Zanetell, J., Fenerty, B., 2021.

Extreme Precipitation across Adjacent burned and Unburned Watersheds reveals Impacts of Low Severity Wildfire on Debris-Flow Processes. J. Geophys. Res. Earth 126 (4), e2020JF005997. https://doi.org/10.1029/2020JF005997.
Menitove, A., 1999. Wildfire-related debris-flow susceptibility in the Santa Monica mountains, Los Angeles and Ventura Counties, California [M.S.]. In: Department of Geology and Geological Engineering, Colorado School of Mines.
Meyer, G.A., Wells, S.G., 1997. Fire-Related Sedimentation events on Alluvial fans, Yellowstone National Park, U.S.a. *SEPM*. J. Sediment. Res. 67. https://doi.org/10.1306/D426863A-2B26-11D7-8648000102C1865D.
Minckley, T.A., Shriver, R.K., Shuman, B., 2012. Resilience and regime change in a southern Rocky Mountain ecosystem during the past 17 000 years. Ecol. Monogr. 82 (1), 49–68. https://doi.org/10.1890/11-0283.1.
Minshall, G.W., Brock, J.T., Varley, J.D., 1989. Wildfires and Yellowstone's Stream Ecosystems. Bioscience 39(10), Article 10. https://doi.org/10.2307/1311002.
Moody, J. A. (2001). *Sediment transport regimes after a wildfire in steep mountainous terrain* (Proceedings of the Seventh Federal Interagency Sedimentation Conference, Reno, NV, pp. X41–X48). http://pubs.usgs.gov/misc/FISC_1947-2006/pdf/1st-7thFISCs-CD/7thFISC/ 7Fisc-V2/7FSC2-10.Pdf#page=43.
Moody, J.A., Martin, D.A., 2001. Initial hydrologic and geomorphic response following a wildfire in the Colorado Front Range. Earth Surf. Process. Landf. 26(10), Article 10. https://doi.org/10.1002/esp.253.
Murphy, B.P., Yocom, L.L., Belmont, P., 2018. Beyond the 1984 Perspective: Narrow Focus on Modern Wildfire Trends Underestimates Future risks to Water Security. *Earth's*. Future 6 (11). https://doi.org/10.1029/2018EF001006. Article 11.
Naiman, R.J., Bechtold, J.S., Drake, D.C., Latterell, J.J., O'Keefe, T.C., Balian, E.V., 2005. Origins, Patterns, and Importance of Heterogeneity in Riparian Systems. In: Lovett, G.M., Turner, M.G., Jones, C.G., Weathers, K.C. (Eds.), Ecosystem Function in Heterogeneous Landscapes. Springer, New York, pp. 279–309. https://doi.org/10.1007/0-387-24091-8_14.
Noske, P.J., Nyman, P., Lane, P.N.J., Rengers, F.K., Sheridan, G.J., 2024. Changes in soil erosion caused by wildfire: a conceptual biogeographic model. Geomorphology 459, 109272. https://doi.org/10.1016/j.geomorph.2024.109272.
O'Sullivan, J.J., Ahilan, S., Bruen, M., 2012. A modified Muskingum routing approach for floodplain flows: Theory and practice. J. Hydrol. 470–471, 239–254. https://doi.org/10.1016/j.jhydrol.2012.09.007.
Pang, B., 1998. River Flood Flow and its Energy loss. J. Hydraul. Eng. 124 (2), 228–231. https://doi.org/10.1061/(ASCE)0733-9429(1998)124:2(228).
Parrett, C., 1987. *Fire-Related Debris Flows in the Beaver Creek Drainage, Lewis and Clark County, Montana* Water Supply Paper 2330. U.S. Geological Survey, pp. 57–67.
Parrett, C., Cannon, S.H., Pierce, K.L., 2004. *Wildfire-Related Floods and Debris Flows in Montana in 2000 and 2001* (Water-Resources Investigations Report 03–4319). U.S, Geological Survey.
Pelletier, J.D., Orem, C.A., 2014. How do sediment yields from post-wildfire debris-laden flows depend on terrain slope, soil burn severity class, and drainage basin area? Insights from airborne-LiDAR change detection. Earth Surf. Process. Landf. 39 (13), 1822–1832. https://doi.org/10.1002/esp.3570.
Piégay, H., Chabot, A., Le Lay, Y.-F., 2020. Some comments about resilience: from cyclicity to trajectory, a shift in living and nonliving system theory. Geomorphology 367, 106527. https://doi.org/10.1016/j.geomorph.2018.09.018.
Pollock, M.M., Beechie, T.J., Jordan, C.E., 2007. Geomorphic changes upstream of beaver dams in Bridge Creek, an incised stream channel in the interior Columbia River basin, eastern Oregon. Earth Surf. Process. Landf. 32 (8), 1174–1185. https://doi.org/10.1002/esp.1553.
Polvi, L.E., Wohl, E., 2013. Biotic Drivers of Stream Planform. BioScience 63 (6), 439–452. https://doi.org/10.1525/bio.2013.63.6.6.
Rengers, F.K., McGuire, L.A., Kean, J.W., Staley, D.M., Dobre, M., Robichaud, P.R., Swetnam, T., 2021. Movement of sediment through a burned landscape: Sediment volume observations and model comparisons in the San Gabriel Mountains, California, USA. J. Geophys. Res. Earth Surf. 126, e2020JF006053.
Riley, K.L., Bendick, R., Hyde, K.D., Gabet, E.J., 2013. Frequency–magnitude distribution of debris flows compiled from global data, and comparison with post-fire debris flows in the western U.S. Geomorphology 191, 118–128. https://doi.org/10.1016/j.geomorph.2013.03.008.
Rodman, K.C., Veblen, T.T., Saraceni, S., Chapman, T.B., 2019. Wildfire activity and land use drove 20th-century changes in forest cover in the Colorado front range. Ecosphere 10 (2), e02594. https://doi.org/10.1002/ecs2.2594.
Roth, H.K., Nelson, A.R., McKenna, A.M., Fegel, T.S., Young, R.B., Rhoades, C.C., Wilkins, M.J., Borch, T., 2022. Impact of beaver ponds on biogeochemistry of organic carbon and nitrogen along a fire-impacted stream. Environ Sci Process Impacts 24 (10), 1661–1677. https://doi.org/10.1039/D2EM00184E.
Ryan, S.E., Shobe, C.M., Rathburn, S.L., Dixon, M.K., 2024. Suspended-sediment response to wildfire and a major post-fire flood on the Colorado Front Range. River Res. Appl. rra.4286. https://doi.org/10.1002/rra.4286.
Santi, P.M., deWolfe, V.G., Higgins, J.D., Cannon, S.H., Gartner, J.E., 2008. Sources of debris flow material in burned areas. Geomorphology 96 (3–4), 310–321. https://doi.org/10.1016/j. geomorph.2007.02.022.
Schumm, S.A., 1956. Evolution of drainage systems and slopes in badlands at Perth Amboy, new Jersey. Geol. Soc. Am. Bull. 67 (5), 597. 10.1130/0016-7606(1956)67[597:EODSAS]2.0.CO;2.
Sear, D.A., Millington, C.E., Kitts, D.R., Jeffries, R., 2010. Logjam controls on channel : floodplain interactions in wooded catchments and their role in the formation of multi-channel patterns. Geomorphology 116 (3–4), 305–319. https://doi.org/10.1016/j.geomorph.2009.11.022.
Searle, S.R., Speed, F.M., Milliken, G.A., 1980. Population marginal Means in the Linear Model: an Alternative to Least Squares Means. Am. Stat. 34 (4), 216–221. https://doi.org/10.1080/00031305.1980.10483031.
Sholtes, J.S., Doyle, M.W., 2011. Effect of Channel Restoration on Flood Wave Attenuation. J. Hydraul. Eng. 137 (2), 196–208. https://doi.org/10.1061/(ASCE)HY.1943-7900. 0000294.
Smith, H., Sheridan, G., Lane, P., Nyman, P., Haydon, S., 2011. Wildfire effects on water quality in forest catchments: a review with implications for water supply. J. Hydrol. 396, 170–192.
Staley, D.M., Negri, J.A., Kean, J.W., Laber, J.L., Tillery, A.C., Youberg, A.M., 2017. Prediction of spatially explicit rainfall intensity–duration thresholds for post-fire debris-flow generation in the western United States. Geomorphology 278, 149–162. https://doi.org/10.1016/j.geomorph.2016.10.019.
Stanford, J.A., Ward, J.V., Liss, W.J., Frissell, C.A., Williams, R.N., Lichatowich, J.A., Coutant, C.C., 1996. A General Protocol for Restoration of Regulated Rivers. Regul. Rivers Res. Manag. 12 (4–5), 391–413. https://doi.org/10.1002/(SICI)1099-1646(199607) 12:4/5<391::AID-RRR436>3.0.CO;2-4.
Thoms, M.C., Piégay, H., Parsons, M., 2018. What do you mean, 'resilient geomorphic systems'? Geomorphology 305, 8–19. https://doi.org/10.1016/j.geomorph.2017.09.003.
Thorn, C.E., Welford, M.R., 1994. The Equilibrium Concept in Geomorphology. Ann. Assoc. Am. Geogr. 84 (4), 666–696. https://doi.org/10.1111/j.1467-8306. 1994.tb01882.x.
Tiedemann, A.R., Conrad, C.E., Dieterich, J.H., Hornbeck, J.W., Megahan, W.F., Viereck, L.A., Wade, D.D., 1979. Effects of Fire on Water. USDA For. Serv. Gen. Tech. Rep. WO-10.
Triantafillou, S., 2024. A Catchment Is More than the Sum of its Reaches: Post-Fire Resilience at Multiple Spatial Scales. Colorado State University.
USDA Forest Service, 2020. Soil Burn Severity Dataset for the CAMERON PEAK Fire occurring on the Arapaho & Roosevelt National Forests/Pawnee National Grassland National Forest: USDS Forest Service raster digital data. USDA Forest Service, Geospatial Technology and Applications Center, BAER Imagery Support Program. https://fsapps.nwcg.gov/afm/baer/download.php.
Veblen, T.T., Donnegan, J.A., 2005. Historical Range of Variability for Forest Vegetation of the National Forests of the Colorado Front Range. USDA Forest Service.
Veblen, T.T., Lorenz, D.C., 1986. Anthropogenic disturbance and recovery patterns in montane forests, Colorado front range. Phys. Geogr. 7 (1), 1–24. https://doi.org/10.1080/02723646.1986.10642278.
Wagenbrenner, J.W., Robichaud, P.R., 2014. Post-fire bedload sediment delivery across spatial scales in the interior western United States. Earth Surf. Process. Landf. 39 (7), 865–876. https://doi.org/10.1002/esp.3488.
Walker, B., Holling, C.S., Carpenter, S.R., Kinzig, A.P., 2004. Resilience, Adaptability and Transformability in Social-ecological Systems. Ecol. Soc. 9 (2), 5 [online] URL: http://www.ecologyandsociety.org/vol9/iss2/art5.
Westbrook, C.J., Cooper, D.J., Baker, B.W., 2006. Beaver dams and overbank floods influence groundwater–surface water interactions of a Rocky Mountain riparian area. Water Resour. Res. 42 (6), 2005WR004560. https://doi.org/10.1029/2005WR004560.
Westerling, A.L., Hidalgo, H.G., Cayan, D.R., Swetnam, T.W., 2006. Warming and earlier Spring increase Western U.S. Forest Wildfire activity. Science 313 (5789), 940–943. https://doi.org/10.1126/science.1128834.
White, D.C., Morrison, R.R., Wohl, E., 2022. Fire and ice: Winter flooding in a Southern Rocky Mountain stream after a wildfire. Geomorphology 413, 108370. https://doi.org/10.1016/j. geomorph.2022.108370.
White, P., Rengers, F.K., Barnhart, K.R., Nelson, P., 2023, May 8. Exploring the Applicability of Radar-based Quantitative Precipitation estimates for Emergency Assessment of Post-Wildfire Debris Flow Hazards in Colorado. In: Sedimentation and Hydrologic Modeling Conference, St. Louis, Missouri, USA.
Wieting, C., Ebel, B.A., Singha, K., 2017. Quantifying the effects of wildfire on changes in soil properties by surface burning of soils from the Boulder Creek critical Zone Observatory. Journal of Hydrology: Regional Studies 13, 43–57. https://doi.org/10.1016/j.ejrh. 2017.07.006.
Wohl, E., 2011. Threshold-induced complex behavior of wood in mountain streams. Geology 39 (6), 587–590. https://doi.org/10.1130/G32105.1.
Wohl, E., 2013. Migration of channel heads following wildfire in the Colorado Front Range, USA. Earth Surf. Process. Landf. 38 (9), 1049–1053. https://doi.org/10.1002/esp.3429.
Wohl, E., 2016. Spatial heterogeneity as a component of river geomorphic complexity. Progress in Physical Geography: Earth and Environment 40 (4), 598–615. https://doi.org/10.1177/0309133316658615.
Wohl, E., Jaeger, K., 2009. A conceptual model for the longitudinal distribution of wood in mountain streams. Earth Surf. Process. Landf. 34 (3), 329–344. https://doi.org/10.1002/esp.1722.
Wohl, E., Lininger, K.B., Scott, D.N., 2018. River beads as a conceptual framework for building carbon storage and resilience to extreme climate events into river management. Biogeochemistry 141 (3), 365–383. https://doi.org/10.1007/s10533-017-0397-7.
Wohl, E., Marshall, A., Scamardo, J., Rathburn, S., 2024b. Biogeomorphic processes, spatial heterogeneity, and river corridor resilience to stand-killing wildfire. In: In, J. L., Florsheim, A.P., O'Dowd, Chin, A. (Eds.), Biogeomorphic Responses to Wildfire in Fluvial Ecosystems. Geological Society of America, pp. 153–176. https://doi.org/10.1130/2024.2562(08).
Wohl, E., Marshall, A.E., Scamardo, J., White, D., Morrison, R.R., 2022. Biogeomorphic influences on river corridor resilience to wildfire disturbances in a mountain stream of the Southern Rockies, USA. Sci. Total Environ. 153321. https://doi.org/10.1016/j. scitotenv.2022.153321.
Wohl, E., Marshall, A.E., Triantafillou, S., Mobley, M., Means-Brous, M., Morrison, R.R., 2024a. Distribution of logjams in relation to lateral connectivity in the River

Corridor. Geomorphology 451, 109100. https://doi.org/10.1016/j.geomorph.2024.109100.
Wohl, E., Rathburn, S., Chignell, S., Garrett, K., Laurel, D., Livers, B., Patton, A., Records, R., Richards, M., Schook, D.M., Sutfin, N.A., Wegener, P., 2017. Mapping longitudinal stream connectivity in the North St. Vrain Creek watershed of Colorado. Geomorpho- logy 277, 171–181. https://doi.org/10.1016/j.geomorph.2016.05.004.
Woltemade, C.J., Potter, K.W., 1994. A watershed modeling analysis of fluvial geomorpho- logic influences on flood peak attenuation. Water Resour. Res. 30 (6), 1933–1942. https://doi.org/10.1029/94WR00323.
Woodward, B., Vorster, A.G., 2022. *Cameron Peak Burn Severity dNBR* [Unpublished Data].
Wu, J., Baartman, J.E.M., Nunes, J.P., 2021. Comparing the impacts of wildfire and meteorological variability on hydrological and erosion responses in a Mediterranean catchment. Land Degrad. Dev. 32 (2), 640–653. https://doi.org/10.1002/ldr.373.